Journal of Economic Interaction and Coordination (2026) 21:429–475
https://doi.org/10.1007/s11403-025-00472-0

RESEARCH

Connecting the dots: how social networks shape macroeconomic expectations

Rafael Kothe[1]

Received: 14 April 2025 / Accepted: 13 December 2025 / Published online: 10 January 2026

Abstract

Standard behavioral frameworks often overlook how social network topology shapes the coordination of inflation expectations. To address this, I build a hybrid agent-based model that integrates "narrative-rooted" heuristics within a standard New Keynesian structural scaffold. In this framework, beliefs evolve through dual channels: performance-based selection (heuristic switching) and social diffusion (DeGroot learning). Simulations across canonical topologies reveal that seeding a target-based narrative in high-centrality nodes compresses forecast dispersion and accelerates convergence. However, a structural trade-off emerges: while performance evaluations dampen distorting narratives, strong social persuasion reduces volatility but simultaneously decouples expectations from economic fundamentals. This occurs because agents prioritize peer alignment over objective data, highlighting the double-edged nature of social networks: they stabilize expectations when credible narratives diffuse through hubs, but sever the link between beliefs and fundamentals when conformity overrides economic signals.

Keywords Expectations · Economic narratives · Network effects · Behavioral macroeconomics · Agent-based modeling · Monetary policy communication

JEL Classification: D84 · D83 · E52 · E71 · D85

1 Introduction

Macroeconomic expectations are socially conditioned (e.g., Carroll 2003; Dräger et al. 2025). Consequently, social networks act as structural conduits for the transmission of economic narratives (Macaulay and Song 2023a; Shiller 2017). While central banks increasingly harness these dynamics to guide expectations (Ter Ellen et al. 2022; Coibion et al. 2020, 2022), the precise mechanism by which

✉ Rafael Kothe
rafael.kothe@uni-bamberg.de

[1] Institute of Economics, University of Bamberg, Bamberg, Germany

network structure amplifies or dampens these signals remains under-explored. This paper abstracts from the semantic richness of narratives to focus on their structural diffusion: narratives are modeled here as stylized, "narrative-rooted" forecasting heuristics, capturing their stabilizing or destabilizing influence in a tractable form.

Existing literature comprises distinct but converging streams. On one side, behavioral macroeconomic models explore heterogeneous beliefs and heuristic switching (Hommes 2013; Lustenhouwer 2021), but typically assume mean-field interactions that ignore network topology. On the other side, econophysics contributions explicitly model opinion dynamics on networks (e.g., Baumann et al. 2021a; Azzimonti and Fernandes 2023), but often lack the feedback loops of a standard monetary policy framework. A distinct gap remains: we lack models that isolate how network topology shapes belief coordination within a canonical stabilization framework.

This paper bridges this gap by addressing the following question: *Under which network topologies does social conformity stabilize inflation expectations, and when does it decouple expectations from economic fundamentals?* To answer this, I build a hybrid agent-based model (ABM) that blends performance-based heuristic switching with DeGroot-style social learning. The framework retains the New Keynesian core as a structural scaffold. Crucially, rather than attempting a fully boundedly rational aggregation of the macrocore, I treat the NK mechanism as a fixed "isolation device" (Mäki 2009). This analytical choice attributes macroeconomic deviations strictly to the interaction between network topology and belief updating, distinguishing the results from models driven by wealth or fiscal frictions (e.g., Hagenhoff et al. 2025).

The simulations yield four main results that directly address the research question. First, regarding *stabilization*, network structure is decisive: seeding the central bank's target-based heuristic in high-centrality nodes (hubs) compresses forecast dispersion and accelerates convergence to the rational benchmark, an effect maximized in scale-free networks. Second, this stabilizing effect is conditional on the persuasion parameter (χ): performance-based learning dampens misinformation at moderate levels, limiting destabilization to regimes of extreme conformity. Third, regarding the risk of *decoupling*, a structural trade-off emerges: while high social persuasion reduces volatility, it simultaneously weakens the correlation between expectations and economic fundamentals. Fourth, impulse response analysis confirms that stronger social conformity shortens the half-life of shock amplification, provided the dominant narrative is anchored to the target. Overall, the findings highlight the double-edged nature of social amplification: it acts as a powerful stabilizer when credible narratives diffuse through hubs, but decouples expectations from reality when conformity overrides economic signals

The remainder of the paper is structured as follows. Section 2 surveys the literature. Section 3 details the model framework and the convex combination of learning mechanisms. Section 4 presents the simulation results on dispersion, topology effects, and impulse responses. Section 5 discusses the implications of the results. Section 6 concludes.

2 Literature review

First, this paper is situated within existing research on bounded rationality, social learning, and expectations. Much theoretical literature formalizes alternatives to the rational expectations assumption by describing the decision-making process of heterogeneous, boundedly rational agents. These approaches often assume that agents cannot comprehend the complexity of the underlying model, following the ideas of Simon (1957) and Selten (1998). Agents are believed to have cognitive limitations that prevent them from processing complex information and developing rational expectations. Empirical evidence from laboratory experiments and survey data supports these cognitive constraints (Branch 2004; Hommes 2011; Pfajfar and Žakelj 2014). Furthermore, recent evidence confirms that these expectations are socially conditioned by peers and media exposure (Carroll 2003; Easaw and Mossay 2015; Dräger et al. 2025), often involving complex hierarchies between first- and higher-order beliefs (Coibion et al. 2021). Instead of optimization, people use heuristics when making decisions under uncertainty (Gigerenzer and Selten 2002; Luan et al. 2019).

The heuristic switching framework used in this study is a popular method for incorporating bounded rationality in macroeconomic models, assuming that agents update their forecasts based on past mistakes (Brock and Hommes 1997, 1998; Branch and McGough 2010). This framework employs a discrete choice model, allowing agents to switch between different expectation heuristics based on their historical predictive accuracy (McFadden 1974; Manski and McFadden 1981).

Similar approaches that merge macroeconomic frameworks with agent-based techniques are frequently used in business cycle models to incorporate heterogeneous expectations (see, e.g., De Grauwe 2011; De Grauwe and Ji 2019, 2020, 2023; De Grauwe and Foresti 2020; Hommes 2013; Hommes et al. 2017; Proaño and Lojak 2020; Hommes and Lustenhouwer 2019a, b; Galanis et al. 2022). These models are also employed: (1) to study the efficiency of micro- and macroprudential measures (e.g., Assenza et al. 2018; Lengnick and Wohltmann 2016); and (2) to analyze the impact of bounded rationality on monetary policy in empirically enriched New Keynesian models (e.g., De Grauwe and Foresti 2023; Gabaix 2020; Jang and Sacht 2022). Anufriev and Hommes (2012) highlight that applying the heuristic switching framework in macroeconomic models can replicate empirical data obtained in laboratory environments. Other studies and laboratory experiments corroborate this, indicating that the expectation formation of economic agents can be modeled as an alternation of simple, heterogeneous forecasting heuristics (Assenza et al. 2014; Pfajfar and Žakelj 2014, 2018).

Second, this paper is situated within the context of Agent-Based Macroeconomics. Earlier macro-agent-based models tended to rely on self-referential decision-making and abstracted from spatial or networked structures (Dawid and Delli Gatti 2018; Steinbacher et al. 2014; Farmer and Foley 2009). However, recent macro-ABM research addresses these limitations by incorporating detailed local interactions among agents. For instance, Rengs et al. (2020); Rengs and Scholz-Wäckerle (2019) underscore the role of localized interactions in driving macroeconomic dynamics

by demonstrating how signaling effects and co-evolutionary processes influence stability. Similarly, evolutionary multi-agent frameworks developed by Dosi et al. (2010, 2009) illustrate that heterogeneous behaviors and adaptive learning can collectively give rise to emergent business cycles. Recent work has sought to integrate these perspectives more tightly with macroeconomic policy analysis (Fagiolo and Roventini 2017).

In contrast, there exists another strand of the literature—particularly in econophysics and financial markets—that leverages network structures explicitly to capture localized interactions, information cascades, and belief contagion (Panchenko et al. 2013; Han and Yang 2013; Khashanah and Alsulaiman 2016; Hatcher and Hellmann 2023; Bertella et al. 2021; Huang et al. 2023; Benhammada et al. 2021; Iori and Mantegna 2018; Clemente et al. 2020). These contributions often focus on opinion dynamics, polarization, and the topology of social influence (Azzimonti and Fernandes 2023; Martins 2008; Baumann et al. 2021a). Indeed, earlier calls by Lux and Westerhoff (2009) and Farmer and Foley (2009) emphasized that ABMs can better capture the interplay of microlevel herding and belief contagion.

This paper contributes to the literature on Agent-Based Macroeconomics by extending the frameworks of De Grauwe (2011); De Grauwe and Ji (2020, 2023) and Hommes and Lustenhouwer (2019a) by explicitly incorporating network dynamics into expectation formation. Rather than neglecting local interactions, the proposed model embeds agents in various network structures, allowing them to switch between different forecasting heuristics based on a discrete choice mechanism (Manski and McFadden 1981). This design integrates the heuristic switching model (Brock and Hommes 1997, 1998) with the opinion dynamics framework of DeGroot (1974). The model updates agents' beliefs using a convex combination of the heuristic switching probability distribution and the DeGroot update rule. This mechanism integrates the agents' internal assessment of predictive performance with the external social influence exerted by their network neighbors. This approach better reflects the interplay between individual belief formation and social influence than models that abstract from network structures, and it is amenable to empirical validation using data from experimental studies (Hommes 2011, 2021; Bao et al. 2021).

Third, this paper relates to the literature on the role of social networks in disseminating information and the importance of narratives in shaping economic expectations (e.g., Bailey et al. 2018; Flynn and Sastry 2024; Andre et al. 2024; Gorodnichenko et al. 2021; Luarn et al. 2014; Bargigli and Tedeschi 2014). These stories often spread virally within social networks, amplifying their impact (Shiller 2017; Beckert 2016; Tuckett and Nikolic 2017; Akerlof and Snower 2016). Roos and Reccius (2024) emphasize the performative nature of narratives, showing how they guide agents' expectations and actions under uncertainty, a notion supported by Tuckett and Tuckett (2011) and MacKenzie (2008), who explore the self-fulfilling power of emotionally charged and model-driven stories. Central banks also leverage narratives to anchor inflation expectations, knowing that effective communication can shift price momentum (Baumann et al. 2021b) or potentially trigger persistent narrative hysteresis" (Flynn and Sastry 2025). Empirical studies further demonstrate how narratives

propagate expectations through social networks (Aral and Walker 2012; Tuckett and Taffler 2012). While heuristic switching models account for some narrative-driven adaptation, they often overlook the explicit mechanisms by which narratives, rooted in "imagined futures" (Beckert and Bronk 2018), shape macroeconomic outcomes (e.g., Hommes 2013; Hommes and Lustenhouwer 2019a). Deeper integration of performative and narrative elements into macroeconomic theory is needed. Recent studies on inflation rates have leveraged social network data to explore policy communication effects (Lamla and Vinogradov 2021), narrative monetary policy surprises (Ter Ellen et al. 2022), and the news-driven transmission of economic narratives (Macaulay and Song 2023a, b). For instance, Larsen et al. (2021) find that media significantly influence inflation expectations and information rigidities, while Beckers et al. (2017) and Sharpe et al. (2023) demonstrate that the semantic properties of economic narratives serve as predictive indicators for economic outcomes.

Fourth, this paper also contributes to the policy-oriented research on central bank communication. The evolution and impact of central bank communication strategies have become important for monetary policy effectiveness and financial stability. Studies have shown that central bank communication can significantly influence market expectations and enhance the predictability of monetary policy decisions (Blinder et al. 2008; Woodford 2005; Coibion et al. 2020, 2022). Best practices for central bank communication have been outlined by institutions like the IMF (2022). Research also explores the impact of central bank communication on financial stability (Born et al. 2014; Cieslak and Schrimpf 2019), showing the importance of clear and consistent communication during periods of unconventional policy to prevent unanchored expectations (Lustenhouwer 2021). Furthermore, the integration of bounded rationality into New Keynesian models provides insights into how central bank communication strategies affect expectations and policy outcomes (Gabaix 2020). Finally, research on the influence of central bank announcements on public beliefs emphasizes the need for clear communication to manage expectations effectively (Lamla and Vinogradov 2019; Blinder et al. 2024; Dräger 2023).

3 Model framework

The model framework retains the standard New Keynesian (NK) three-equation system, comprising the IS curve, the Phillips curve, and a Taylor-type rule, as the structural core. I explicitly acknowledge the epistemological tension inherent in this hybrid design: the NK IS curve is traditionally derived from the intertemporal optimization of a representative rational agent, whereas the agents in this model employ boundedly rational forecasting heuristics.

Recent literature has sought to resolve this inconsistency by re-deriving aggregate demand directly from the Euler equations of heterogeneous boundedly rational agents (e.g., Hagenhoff et al. 2025; Massaro 2013). While such microfoundations provide internal consistency, they yield aggregate laws of motion that differ structurally from the canonical NK baseline. These derivations often introduce backward-looking consumption dynamics or long-horizon forecasts that fundamentally alter the transmission mechanism.

This paper prioritizes, however, comparability over full microfoundational closure. I deliberately employ the standard NK scaffold as an isolation device in the sense of Mäki (2009, p. 30), utilizing its idealizations to "control for noise" by bracketing the confounding wealth and fiscal dynamics that arise in more complex, fully microfounded aggregations. This allows me to isolate the specific behavioral mechanism of interest: the interaction between network topology and social persuasion.

This approach aligns with the established tradition of behavioral New Keynesian heuristics (e.g., De Grauwe 2011; Hommes and Lustenhouwer 2019a; De Grauwe and Ji 2023; Proaño and Lojak 2020). These studies similarly employ the NK structure not as a behavioral ground truth, but as a fixed laboratory benchmark to facilitate direct comparison with established literature.

In this setup, "narratives" are operationalized as compact, quantitative heuristics for expectation formation: stylized belief rules whose prevalence evolves socially through network interactions. They are not modeled as content-rich stories in the sense of narrative economics (Shiller 2017; Beckert and Bronk 2018; Tuckett and Taffler 2012); rather, they function as transmissible forecasting rules whose diffusion over the trust network shapes aggregate expectations. This abstraction keeps the model tractable while capturing the functional role narratives play in expectation coordination.

To guide the reader through the model architecture, Fig. 1 provides a schematic overview of the initialization, microbehavioral updates, and macrolevel feedback loops formalized in the following subsections.

3.1 The economy

The behavioral macroeconomic model proposed by De Grauwe (2011) and further developed by De Grauwe and Ji (2020, 2023) forms the foundation of this approach. This model extends the New Keynesian business cycle framework presented by Galí (2008) by incorporating heterogeneous forecasting rules.

The demand side of the economy is represented by the New Keynesian IS curve:

$$x_t = a_1 \tilde{E}_t(x_{t+1}) + (1 - a_1)x_{t-1} - a_2(i_t - \tilde{E}_t(\pi_{t+1})) + \epsilon_t^x \tag{1}$$

Here, x_t denotes the output gap, i_t the nominal interest rate, $\tilde{E}_t(x_{t+1})$ the expected output gap, and $\tilde{E}_t(\pi_{t+1})$ the expected inflation rate. The parameter a_2 represents the inverse elasticity of substitution of demand, and the tilde ($\tilde{E}_t$) indicates bounded rational expectations (BRE).

The supply side of the economy is described by the New Keynesian Phillips curve (NKPC), which relates the inflation rate (π_t) to the output gap (x_t) and the expected future inflation rate ($\tilde{E}_t(\pi_{t+1})$):

$$\pi_t = b_1 \tilde{E}_t(\pi_{t+1}) + (1 - b_1)\pi_{t-1} + b_2 x_t + \epsilon_t^\pi \tag{2}$$

In this equation, b_2 represents the slope of the Phillips curve, indicating the extent to which inflation adjusts to changes in the output gap and how flexible firms are

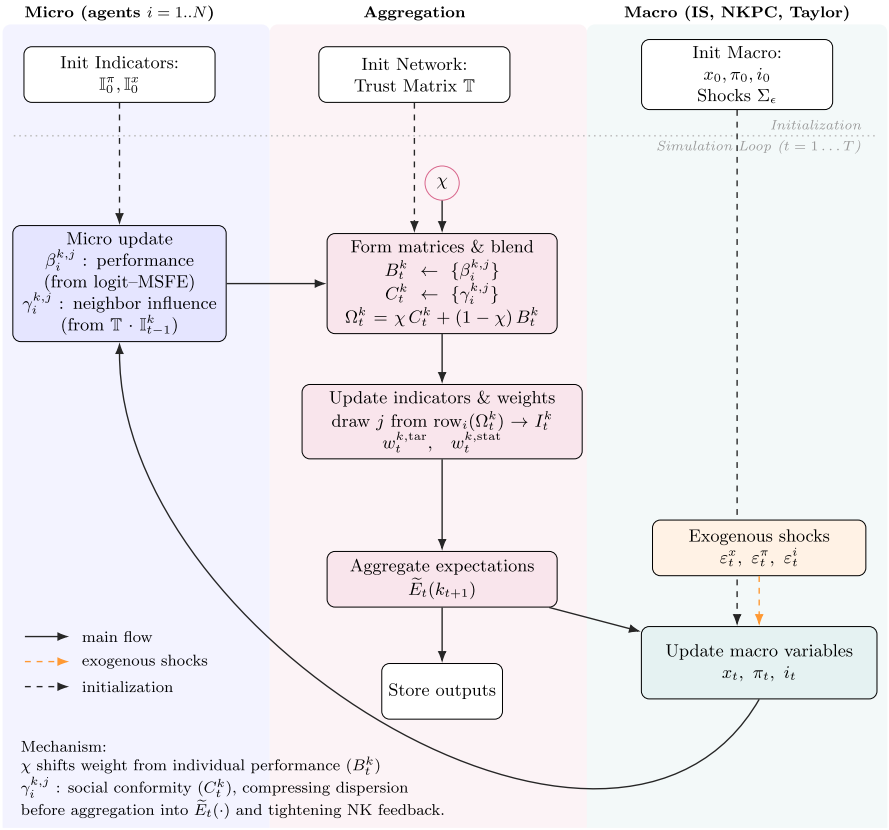

Fig. 1 Schematic overview of the model's three-layer architecture. The top row shows the initialization of agents, network topology, and macrovariables. The simulation loop (vertical lanes) illustrates the sequence: (**i**) Microlevel update of performance and social influence; (**ii**) aggregation via the persuasion operator Ω_t^k; and (**iii**) macrolevel update via the IS-NKPC-Taylor block (the isolation device). See Algorithm 2 for detailed pseudo-code

in their price-setting behavior. Following De Grauwe and Ji (2020, 2023), lagged output is included in the demand equation, and lagged inflation is included in the supply equation.

The central bank's response to fluctuations in the inflation rate and the output gap is modeled by the Taylor rule:

$$i_t = (1 - c_3)[c_1(\pi_t - \pi^*) + c_2 x_t] + c_3 i_{t-1} + \epsilon_t^i \tag{3}$$

According to this equation, the central bank raises interest rates if the output gap widens or if observed inflation rises relative to the target inflation rate. The central bank also smooths the interest rate by considering the lagged interest rate (i_{t-1}), measured by the coefficient c_3.

Noise terms are added to Eqs. (1), (2), and (3) to represent the exogenous shocks affecting the economy. These noise terms (ϵ_t^x, ϵ_t^π, and ϵ_t^i) follow a white-noise process

and are assumed to be normally distributed random variables with a zero mean and constant standard deviations (σ^x, σ^π, and σ^i), e.g., $\epsilon_t^x \sim N(0, \sigma^x)$, $\epsilon_t^\pi \sim N(0, \sigma^\pi)$, and $\epsilon_t^i \sim N(0, \sigma^i)$.

3.2 Narrative-rooted forecasting heuristics

The heuristic switching framework, rooted in Brock and Hommes (1997), captures how boundedly rational agents adapt their expectations by dynamically choosing between two stylized belief rules, based on past performance. These rules are not narratives in the rich sense of Shiller (2017), Beckert (2016), or Tuckett and Tuckett (2011), which emphasize dynamic, emotionally resonant, and socially constructed stories that evolve over time. Rather, they are narrative-rooted heuristics: simplified forecasting devices that abstractly represent the stabilizing or destabilizing influence such narratives can exert on expectations. The specific forms follow De Grauwe and Ji (2020, 2023). The target-based heuristic reflects a stabilizing narrative of central bank credibility, in which agents expect inflation to return to target (π^* at $t+1$) and the output gap to close (i.e., $x = 0$). By contrast, the naive heuristic proxies destabilizing or conflicting narratives, operationalized as simple extrapolation from past outcomes. In this way, the framework embeds narrative influence in a tractable heuristic form, enabling analysis of how their diffusion through social networks shapes macroeconomic stability without modeling narrative content or evolution. The degree of central bank credibility is proxied by the share of targeters, i.e., agents who trust the announced target π^*. These agents apply the following heuristic to forecast:

$$\tilde{E}_t^{\text{tar}}(x_{t+1}) = 0 \tag{4}$$

$$\tilde{E}_t^{\text{tar}}(\pi_{t+1}) = \pi^* \tag{5}$$

Agents using naive (or static) expectations forecast the next period's value by simply employing the previous period's observation (De Grauwe and Ji 2020, 2023; Lengnick and Wohltmann 2016). Therefore, they use Eq. 6 as a forecasting rule:

$$\tilde{E}_t^{\text{stat}}(k_{t+1}) = k_{t-1} \quad \text{with} \quad k \in \{\pi, x\} \tag{6}$$

Following Schmitt (2021), agent i's choice of heuristic j from the set of forecasting heuristics $\{\text{tar}, \text{stat}\}$ for forecasting variable $k \in \{\pi, x\}$ can be formalized by:

$$\tilde{E}_{i,t}(k_{t+1}) = \begin{cases} \tilde{E}_{i,t}^{\text{tar}}(k_{t+1}) & \text{if} \quad I_i^k(t) = 1 \\ \tilde{E}_{i,t}^{\text{stat}}(k_{t+1}) & \text{if} \quad I_i^k(t) = 0 \end{cases} \tag{7}$$

Agent i will opt for $\tilde{E}_{i,t}^{\text{tar}}(k_{t+1})$ if its indicator function assumes the value 1 and for $\tilde{E}_{i,t}^{\text{stat}}(k_{t+1})$ otherwise. Defining $\omega_i^{k,\text{tar}}(t)$ and $\omega_i^{k,\text{stat}}(t)$ as the switching probabilities that govern agent i's choice of heuristic $j \in \{\text{tar}, \text{stat}\}$ when forecasting variable $k_{t+1} \in \{\pi, x\}$ in period t, the indicator function can be formalized by:

$$I_i^k(t) = \begin{cases} \lambda_i^{k,\text{tar}}(t) = 1, \text{ with prob } \omega_i^{k,\text{tar}}(t) \\ \lambda_i^{k,\text{tar}}(t) = 0, \text{ with prob } \omega_i^{k,\text{stat}}(t) \end{cases} \quad \forall_{i\in\{1,\ldots,N\}} \tag{8}$$

The indicator matrix $\mathbb{I}_t^k = \{0,1\}^{N\times 2}$ indicating the forecasting choice of all agents is shown in Appendix A.1.

The number of agents that follow each forecasting rule can now easily be defined by:

$$n_t^{k,\text{tar}} = \sum_{i=1}^{N} \lambda_i^{k,\text{tar}}(t) \tag{9}$$

$$n_t^{k,\text{stat}} = \sum_{i=1}^{N} |\lambda_i^{k,\text{tar}}(t) - 1| \tag{10}$$

Finally, the relative number of agents that follow each forecasting heuristic is defined by:

$$w_t^{k,\text{tar}} = \frac{n_t^{k,\text{tar}}}{N} \tag{11}$$

$$w_t^{k,\text{stat}} = \frac{n_t^{k,\text{stat}}}{N} \tag{12}$$

The relative numbers of agents sum to one, so $w_t^{k,\text{tar}} = 1 - w_t^{k,\text{stat}}$.

After setting up the expectation heuristics and specifying the selection mechanism, the conditional expectation operator in Eqs. 1 and 2 is replaced by the weighted average of expectation heuristics, using the respective proportions $w_t^{k,j}$ to derive the market expectations (Arifovic et al. 2013; Brazier et al. 2008):

$$\begin{aligned} \tilde{E}_t(k_{t+1}) &= w_t^{k,\text{tar}} \tilde{E}_t^{\text{tar}}(k_{t+1}) + w_t^{k,\text{stat}} \tilde{E}_t^{\text{stat}}(k_{t+1}) \\ &= w_t^{k,\text{tar}} k^* + w_t^{k,\text{stat}} k_{t-1} \end{aligned} \tag{13}$$

Based on the share of agents given by Eqs. (11) and (12), the optimistic or pessimistic market sentiments can now be formally depicted. The definition of market sentiments is again based on De Grauwe and Ji (2020, 2023) and works as follows:

$$S_t = \begin{cases} w_t^{k,\text{stat}} - w_t^{k,\text{tar}} & \text{if } k_{t-1} > 0 \\ -w_t^{k,\text{stat}} + w_t^{k,\text{tar}} & \text{if } k_{t-1} < 0 \end{cases} \tag{14}$$

where S_t is the index of market sentiment, defined in Eq. (14), ranging from -1 (purely deflationary expectations) to $+1$ (purely inflationary expectations), and $k \in \{\pi, x\}$.

3.3 Switching mechanism based on performance adaptation

The selection of a forecasting heuristic is governed by a discrete-choice approach (McFadden 1974), where agents assess the historical predictive accuracy of each heuristic using the Mean Squared Forecast Error (MSFE), which has been applied in prior research (e.g., Branch and McGough 2010; De Grauwe and Ji 2020, 2023; Lengnick and Wohltmann 2016).

The attractiveness of heuristic $j \in \{\text{tar}, \text{stat}\}$ for variable $k \in \{\pi, x\}$ in period $t$is defined as:

$$A_t^{k,j} = -(k_{t-1} - \tilde{E}_{t-2}^{j}(k_{t-1}))^2 + \zeta A_{t-1}^{k,j} \tag{15}$$

with $k \in \{\pi, x\}$ and $j \in \{\text{tar}, \text{stat}\}$

where ζ is a memory parameter determining how much weight agents assign to past forecast errors (Franke and Westerhoff 2018). A higher ζ indicates longer memory, reinforcing persistence in heuristic choice.

The probability that an agent selects a specific forecasting heuristic j for variable k in period t is determined by the multinomial logit model (Branch and McGough 2010):

$$\beta_t^{k,j} = \frac{\exp\{\theta A_t^{k,j}\}}{\sum_{j'} \exp\{\theta A_t^{k,j'}\}} \tag{16}$$

with $k \in \{\pi, x\}$ and $j \in \{\text{tar}, \text{stat}\}$

where θ is the intensity of choice parameter, governing how strongly agents react to differences in performance. When θ is high, agents switch heuristics more frequently in response to performance differentials; when θ is low, agents are more inertial and less sensitive to past forecast errors.

This heuristic switching framework allows agents to dynamically adapt their expectations based on observed economic conditions and better captures the heterogeneity observed in empirical inflation expectation surveys (Pfajfar and Žakelj 2014). Moreover, the framework aligns with evidence suggesting that households and firms frequently adjust their forecasting rules based on past forecast errors rather than forming fully rational expectations (Branch and McGough 2010).

Assuming $\beta_i^{k,\text{tar}}(t) = \beta^{k,\text{tar}}(t)$ and $\beta_i^{k,\text{stat}}(t) = \beta^{k,\text{stat}}(t)\ \forall\, i$, these probabilities represent the choices of agent i for heuristics j. Let the switching probabilities matrix (SPM) be defined as $\mathbb{B}_t^k$. The SPM is provided in matrix notation in Appendix A.2 for reference.

3.4 Network structures and agent connectivity

The agent population consists of $N = 100$ agents, embedded in alternative network structures that capture distinct characteristics of real-world communication (see Table 1). Reported values correspond to averages over 1000 random seeds. While clustering and path-length statistics vary slightly across runs, edge counts and mean

Table 1 Structural properties of the four network types (BA, ER, NWS, REG) used in the simulations (for $N = 100$)

Type	BA	ER	NWS	REG
Nodes N	100	100	100	100
Edges E	1056	1200	1490	3000
Density δ	0.213	0.242	0.301	0.606
Avg. degree	21.12	24.00	29.80	60.00
Avg. clustering	0.315	0.243	0.546	0.598
Diameter	3	3	3	2
Avg. shortest path	1.80	1.76	1.71	1.39

Reported values are averages over 1000 independent seeds. Each topology preserves its canonical features while spanning low to high edge density δ. For BA and REG, the number of edges and the mean degree are deterministic given the parameters, so seed variation affects only higher-order statistics (e.g., clustering, path lengths). For ER, the exact edge count is fixed by construction in the $G(n, M)$ variant, leaving little scope for variation across seeds. For NWS, shortcut placement introduces randomness, so edge counts and clustering fluctuate across runs, but converge to stable averages. This procedure serves as a first sensitivity analysis, showing that the qualitative comparative statics are robust to seed variation

degrees are fixed by construction in Barabási–Albert, Erdős–Rényi, and Regular graphs, leaving only Newman–Watts–Strogatz with stochastic variation, (see table note for details). The Barabási–Albert network (BA) averages $E \approx 1056$ edges (mean degree $\bar{d} \approx 21.1$, density $\delta \approx 0.21$), preserving hub dominance, short path lengths, and moderate clustering (well below the small-world and regular cases). The Newman–Watts–Strogatz small-world network (NWS), with an average of $E \approx 1490$ edges ($k = 24$, $p \approx 0.24$), exhibits high clustering with short path lengths (comparable to BA/ER at this calibration). This structure supports efficient diffusion while maintaining neighborhood coherence, making it well-suited for modeling localized economic interactions such as household consumption or firm-level price-setting (Easaw and Mossay 2015; Jackson et al. 2008; Carvalho 2014), while also allowing local shocks to escalate to the macrolevel (Acemoglu et al. 2012; Baqaee and Farhi 2019). The Erdős–Rényi random graph (Erdos et al. 1960), fixed at $E = 1200$ edges (mean degree $\bar{d} = 24$, density $\delta \approx 0.24$), serves as a neutral benchmark with a Poisson degree distribution, low clustering, and short paths, highlighting how dynamics unfold in the absence of systematic structure. By contrast, the random regular network (REG) (Newman 2003), with $E = 3000$ edges and uniform degree $d = \bar{d} = 60$, enforces perfect degree homogeneity. While not an empirical analogue, this structure preserves a useful counterfactual benchmark: at high density ($\delta \approx 0.61$), it effectively realizes a "ceiling case" for persuasion-driven conformity (e.g., the maximal speed of belief convergence) due to the enlarged spectral gap (or minimized SLEM) in dense regular graphs, which governs consensus rate under DeGroot-type dynamics (Boyd et al. 2004; Olfati-Saber and Murray 2004; Golub and Jackson 2010). In practice, edge counts and mean degrees are deterministic in BA, ER, and REG, leaving only NWS with stochastic edge realizations around a stable mean (see Table 1).

Given these constraints, I harmonize N and select parameters such that BA and ER match the target scaling, NWS falls in an adjacent (slightly denser) band due to shortcut placement, and REG is intentionally set to a much higher density as a "ceiling" case. Formally, I scale the target number of edges with system size as $E^(N) = 12N$, which implies a reference mean degree $\bar{d}^=24$ at $N = 100$. This target is matched exactly in ER, approximated in BA, exceeded in NWS, and deliberately doubled in REG ($\bar{d} = 60$). The baseline of $N = 100$ balances computational tractability with sufficient heterogeneity in centrality and neighborhoods. In DeGroot-style averaging, convergence largely hinges on the spectrum of the row-stochastic matrix (mixing) rather than N *per se* (see, e.g., Golub and Jackson 2010, 2012; Jadbabaie et al. 2012). The realized statistics confirm that these canonical features are preserved across seeds and N, ensuring comparability for the analysis. This calibration is robust across different network sizes (see robustness footnote for $N \in 100, 300, 500$).[1]

Interpreting E (and thus δ) as a reduced-form proxy for communication intensity provides a mapping to empirical settings. Given unweighted ties, E proxies potential contact opportunities rather than frequency or tie strength. Hub-dominated diffusion in scale-free graphs parallels the role of media outlets or financial "super-spreaders", consistent with evidence from large-scale communication networks that exhibit hub dominance and power-law degree distributions (Onnela et al. 2007; Barabási 2009). Small-world graphs resemble community-based or professional networks, where dense local ties coexist with occasional long-range connections, a structure documented in empirical studies of collaboration and social networks (Watts and Strogatz 1998; Amaral et al. 2000; Uzzi and Spiro 2005). Erdős–Rényi graphs serve as a theoretical baseline for unstructured connections in diffusion models (Newman 2003). Random regular networks approximate egalitarian peer exchanges, functioning mainly as counterfactual benchmarks in comparative analyses (Jackson et al. 2008).

Table 1 illustrates these four canonical structures, making the calibration and their structural contrasts transparent. These networks are deliberately stylized abstraction devices rather than empirical reconstructions. Extensions include incorporating homophily, where connections form conditional on agent traits (see, e.g., Currarini et al. 2016), and combining theory-driven abstractions with empirical network data to reduce biases and strengthen validity (see, e.g., Will et al. 2020). Such extensions would complement the present comparative statics focus on structural

[1] While a full grid over (N, δ) lies beyond scope, I conducted robustness checks for $N \in \{100, 300, 500\}$ using the same parametrization rules ($E^*(N) = 12N$) and averaging outcomes across 100 random seeds per case. Holding the average degree $\bar{d}$ (and thus density $\delta = \bar{d}/(N-1)$ for fixed N) approximately constant across models (BA: $m \approx \bar{d}/2$, yielding $\bar{d} \approx 2m$ up to small finite-N corrections; ER $G(n, M)$: $M \approx N\bar{d}/2$; NWS: $k \approx \bar{d}$ with small p; REG: $d = \bar{d}$ with Nd even, so that d and $\bar{d}$ coincide by construction) ensures comparability. As expected, edge counts, density, and mean degree are deterministic in BA, ER, and REG, while only NWS exhibits stochastic variation in realized E across seeds. Averaging therefore yields stable structural benchmarks, with residual variation limited to clustering and path-length metrics. Importantly, these changes refine the distribution of centrality without altering the qualitative comparative statics: across N, all networks remain connected, retain their canonical features (hub dominance in BA, Poisson-like degree spread in ER, high clustering in NWS, homogeneity in REG), and preserve mixing properties relevant for DeGroot-type convergence. Detailed sensitivity tables are omitted to maintain focus on the main results.

archetypes and communication intensity. These calibrated structures therefore provide a controlled testbed for evaluating how connectivity shapes belief dynamics under DeGroot-style averaging, which is the focus of the subsequent analysis.

3.5 Social influence and belief updating

Individuals, due to cognitive limitations, partially rely on information from their social network when making decisions under uncertainty (Azzimonti and Fernandes 2023). This phenomenon, known as informational social influence, can be illustrated using the DeGroot model (Buechel et al. 2015). The DeGroot model (DeGroot 1974) represents how agents update their beliefs through interactions with their network neighbors, combining their own opinions with those of their peers. Experimental and empirical evidence suggests that individuals tend to adhere to this heuristic learning process (e.g., Chandrasekhar et al. 2020; Choi et al. 2008; Corazzini et al. 2012). The DeGroot-type linear updating setting applied here uses an average-based updating process for belief dynamics, where agents' choice of forecasting rule is influenced by individual performance metrics derived from past economic outcomes (k_{t-1}) and the actions (heuristic choices) of their network neighbors in the previous period. Hence, agents update their opinions quasi-naively to a probability distribution that better fits the decisions made in their network vicinity.

All networks can be characterized by a row-stochastic $n \times n$ matrix denoted by

$$\mathbb{T} = (g_{ij})_{i,j=1}^{n},$$

where for all $i, j \in N$, we have $g_{ij} \geq 0$ and $\sum_{j=1}^{n} g_{ij} = 1$. Here, g_{ij} represents the weight that agent i assigns to agent j's current belief when updating their own belief in the next period. This matrix, which is herein called trust matrix (TM), encapsulates the network topology and the intensity of trust among agents.

Assuming symmetric trust (i.e., $g_{ij} = g_{ji}$), reflecting reciprocal confidence between agents, the TM is defined explicitly as:

$$\mathbb{T} = \begin{bmatrix} g_{11} & g_{12} & \cdots & g_{1n} \\ g_{21} & g_{22} & \cdots & g_{2n} \\ \vdots & \vdots & \ddots & \vdots \\ g_{n1} & g_{n2} & \cdots & g_{nn} \end{bmatrix}. \tag{17}$$

The row-stochastic property ensures that each row sums to 1, which enables a clear probabilistic interpretation of the trust levels: each agent distributes a total weight of 1 across all other agents' beliefs. This structure is crucial for modeling how information and influence propagate through the network.

The social influence of neighbors' decisions is measured by a matrix derived from the inner product of this TM (17) and the indicator matrix (IM) provided in Appendix A.1 for variable k from period $t-1$. The resulting conformity probabilities matrix (CPM) for variable k in period t is then given by (see Appendix A.3 for details):

$$CPM_t^k = \mathbb{C}_t^k = \mathbb{T} \cdot \mathbb{I}_{t-1}^k \tag{18}$$

In addition, agents' individual past forecasting performance is captured by the discrete-choice-based model, yielding the switching probabilities matrix given in Appendix A.2. The core part of the model is a convex combination of these two probability distributions. The probability distributions over a discrete set of alternatives are weighted by a persuasion parameter and additively combined to create the weighted probabilities matrix (wPM):

$$wPM_t^k = \Omega_t^k = \chi \cdot \mathbb{C}_t^k + (1-\chi) \cdot \mathbb{B}_t^k. \tag{19}$$

Here, each element $\omega_i^{k,j}(t)$ of Ω_t^k represents the probability that agent i opts for heuristic $j \in \{\text{tar}, \text{stat}\}$ to forecast the variable $k_{t+1} \in \{\pi, x\}$ in period t, as given mathematically by:

$$\omega_i^{k,j}(t) = \chi \cdot \left(\sum_{l=1}^{n} g_{il} \lambda_l^{k,j}(t-1) \right) + (1-\chi) \cdot \left(\frac{\exp\{\theta A_i^{k,j}(t)\}}{\sum_{j'} \exp\{\theta A_i^{k,j'}(t)\}} \right) \tag{20}$$

This formulation combines two components. The first term, $\sum_{\ell=1}^{N} g_{i\ell}\, \lambda_\ell^{k,j}(t-1)$ (weighted by χ), captures DeGroot-style social influence: $g_{i\ell}$ is the trust weight agent i assigns to neighbor ℓ, and $\lambda_\ell^{k,j}(t-1)$ indicates neighbor ℓ's previous heuristic choice. The second term, weighted by $1-\chi$, is a multinomial logit probability based on past performance, measured by mean squared forecast error (MSFE), with θ controlling responsiveness. The persuasion parameter χ therefore acts as a convex combination weight: $\chi = 0$ yields pure individual learning (logit–MSFE switching), $\chi = 1$ yields pure social learning (DeGroot), and intermediate values blend the two in the weighted probabilities matrix Ω_t^k. Equations 18–20 imply the following mechanism: when highly central nodes coordinate on the target heuristic, the conformity term $\mathbb{T} \cdot \mathbb{I}_{t-1}^k$ concentrates probability mass on 'tar' across neighborhoods. For $0 < \chi < 1$, the weighted operator Ω_t^k tilts individual logit choices toward 'tar' even when MSFE differentials are modest, thereby compressing cross-sectional dispersion before aggregation into $\widetilde{E}_t(\cdot)$. Because Ω_t^k blends conformity and performance ($\chi C_t^k + (1-\chi)B_t^k$), higher χ reduces forecast dispersion before aggregation into $\widetilde{E}_t(\pi_{t+1})$ and $\widetilde{E}_t(x_{t+1})$. With more homogeneous expectations feeding the IS and NKPC blocks, the feedback loop tightens and convergence to the RE path is faster under the same Taylor rule. Conversely, a naive narrative amplifies macrodeviations only when χ is sufficiently high to override MSFE-based inertia. For reference, Appendix A.4 details the construction of Ω_t^k, and Appendix C.1 summarizes the linear solution notation.

The conformity channel in eqs. 18–20 adopts a linear DeGroot operator with a homogeneous persuasion parameter χ and intensity of choice θ. This transparent baseline isolates the role of interaction in compressing dispersion. However, it deliberately abstracts from richer contagion mechanisms, such as bounded-confidence dynamics (Hegselmann and Krause 2002; Lorenz 2007), threshold-based adoption

(Granovetter 1978), or identity-driven contagion.[2] Furthermore, the model abstracts from deep agent heterogeneity by assuming homogeneous persuasion propensities (χ_i) and intensities of choice (θ_i) across agents.

A minimal robustness extension would relax homogeneity by specifying

$$\Omega_t^k = \mathrm{diag}(\chi)\, C_t^k + \big(I - \mathrm{diag}(\chi)\big) B_t^k,$$

so that agents with higher χ_i place more weight on social conformity while others rely more on individual performance. The aggregation operator remains unchanged, but heterogeneous χ_i would amplify the role of network centrality in convergence. We assume symmetric trust and homogeneous $\beta_i^{k,j}(t)$ across i (see Appendix A.2) to isolate the role of network structure and χ before introducing richer heterogeneity. More complex extensions (including bounded-confidence DeGroot, nonlinear update rules, or heterogeneity in θ_i) are left for future work.

3.6 Simulation design

Building on the definitions in the previous Sect. 3.5, the computational framework follows the three-layer structure outlined in Fig. 1. At the microlevel, Algorithm 1 specifies how each agent updates heuristic attractiveness based on past forecast errors, forms switching probabilities, and incorporates social influence from neighbors. At the aggregation level, individual probabilities are collected into matrices B_t^k and C_t^k, which are combined through the persuasion operator Ω_t^k (Eq. 19). This produces updated indicator matrices and aggregate weights that yield market expectations $\widetilde{E}_t(\cdot)$. At the macrolevel, these expectations feed into the IS curve, the New Keynesian Phillips curve, and the Taylor rule, together with exogenous shocks. The NK block is retained as a tractable comparative baseline; the novelty of the framework lies in how the persuasion operator Ω_t^k reshapes expectations before they enter IS–NKPC–Taylor dynamics. Matrix objects (the switching probability matrix $\mathbb{B}_t^k$, conformity matrix $\mathbb{C}_t^k$, and weighted matrix Ω_t^k) are defined in Appendices A.2 and A.3; the linear solution notation is summarized in Appendix C.1. The complete algorithmic details remain available in Appendix B for replication. As noted in 3.5, the persuasion operator Ω_t^k is specified as a linear DeGroot mechanism with homogeneous parameters; this baseline is retained here to highlight the aggregation pipeline rather than alternative diffusion dynamics.

[2] Bounded-confidence models assume agents only update when neighbors' opinions lie within a tolerance band, generating clustering and polarization; threshold models posit that adoption occurs once the share of adopters exceeds an individual-specific threshold, creating nonlinear cascades; identity-driven contagion emphasizes that adoption is more likely when information or behaviors spread within salient social groups.

Algorithm 1 Single Agent Expectation Formation Process

Require: Agent i's information at time t:

- Previous observation k_{t-1} and forecast $E^j_{t-2}(k_{t-1})$ for each heuristic $j \in \{\text{tar}, \text{stat}\}$.
- Previous attractiveness $A^{k,j}_{t-1}$ for each heuristic.
- Parameters: memory ζ, intensity θ, persuasion weight χ.
- For each neighbor $l \in N(i)$: trust weight g_{il} and past choice indicator $\lambda^{k,j}_l(t-1)$.
- Target value k^* (e.g. π^* for inflation or 0 for output).

Ensure: Agent i's forecast $E_{i,t}(k_{t+1})$ for variable k.

1: **for all** $j \in \{\text{tar}, \text{stat}\}$ **do**

2: Compute forecast error: $\text{error}^j \leftarrow k_{t-1} - E^j_{t-2}(k_{t-1})$.

3: Update attractiveness:

$$A^{k,j}_t \leftarrow -\left(\text{error}^j\right)^2 + \zeta\, A^{k,j}_{t-1}$$

4: Compute switching probability (individual component):

$$\beta^{k,j}_t \leftarrow \frac{\exp\{\theta\, A^{k,j}_t\}}{\exp\{\theta\, A^{k,\text{tar}}_t\} + \exp\{\theta\, A^{k,\text{stat}}_t\}}$$

5: **end for**

6: Compute social influence for each heuristic:

$$\gamma^{k,j}_i(t) \leftarrow \sum_{l \in N(i)} g_{il}\, \lambda^{k,j}_l(t-1)$$

7: Combine individual and social components:

$$\omega^{k,j}_i(t) \leftarrow \chi\, \gamma^{k,j}_i(t) + (1-\chi)\, \beta^{k,j}_t, \quad j \in \{\text{tar}, \text{stat}\}$$

8: Normalize $\omega^{k,j}_i(t)$ so that $\omega^{k,\text{tar}}_i(t) + \omega^{k,\text{stat}}_i(t) = 1$.

9: Randomly choose heuristic j^* using the probabilities $\omega^{k,j}_i(t)$.

10: **if** $j^* = \text{tar}$ **then**

11: Set forecast: $E_{i,t}(k_{t+1}) \leftarrow k^*$.

12: **else**

13: Set forecast: $E_{i,t}(k_{t+1}) \leftarrow k_{t-1}$.

14: **end if**

15: **return** $E_{i,t}(k_{t+1})$.

4 Simulation results

Building upon the agent-based model with heterogeneous expectations and network structures, this section presents the computational results from Monte Carlo simulations detailed in Sect. 3.6 to analyze the impact of social influence on inflation expectations and market sentiment, guided by the parameter calibration outlined

Table 2 Parameter values of the calibrated model

Calibration	
Parameter	Description
$a_1 = 0.5$	Coefficient of expected output in IS equation (Smets and Wouters 2003)
$a_2 = 0.2$	Inverse elasticity of substitution (Clarida et al. 2000)
$b_1 = 0.5$	Coefficient of expected inflation in PC equation (Smets and Wouters 2003)
$b_2 = 0.05$	Phillips curve coefficient of the output gap (De Grauwe and Ji 2023)
$c_1 = 1.5$	Interest rate control parameter for inflation (Blattner and Margaritov 2010)
$c_2 = 0.5$	Interest rate control parameter for output (Blattner and Margaritov 2010)
$c_3 = 0.5$	Interest smoothing parameter in Taylor equation (Blattner and Margaritov 2010)
$\pi^* = 0$	Inflation target (De Grauwe and Ji 2023)
$\sigma^x = 0.5$	Standard deviation of the output gap (De Grauwe and Ji 2023)
$\sigma^\pi = 0.5$	Standard deviation of the inflation rate (De Grauwe and Ji 2023)
$\sigma^i = 0.5$	Standard deviation of the nominal interest rate (De Grauwe and Ji 2023)
$\theta = 2$	Intensity of choice (De Grauwe and Ji 2023)
$\zeta = 0.5$	Memory parameter (De Grauwe and Ji 2023)
$\chi \in [0, 1]$	Persuasion parameter (own calibration)

in Table 2 and the network topologies described in Sect. 3.4. Results below reflect the mechanism in Sect. 3.5: $\mathbb{T} \cdot \mathbb{I}^k_{t-1}$ concentrates probability mass on the heuristic adopted by hubs, and χ controls how strongly Ω^k_t translates that into aggregate beliefs. See Eqs. 18-020.

4.1 Parameterization and calibration

Behavioral economic models incorporating evolutionary switching between heterogeneous expectations are complex, often precluding analytical solutions due to their nonlinear dynamics (Hommes 2013).[3] Consequently, this study employs an agent-based Monte Carlo simulation framework to capture local interactions within a heterogeneous expectations environment under bounded rationality. At the outset of each simulation, agents are randomly assigned to follow either the target-based or naive expectation heuristic with equal probability (i.e., a 50:50 split), thereby ensuring an initially balanced heterogeneity in forecasting behavior. To mitigate the influence of transient dynamics, a burn-in period of 30 periods is implemented, during which no data are recorded. This approach ensures that the statistical analysis is not biased by initial conditions. Each simulation run spans 200 periods, with economic shocks modeled as normally distributed random variables with a mean of zero and

[3] For an in-depth discussion on the stability conditions of behavioral models, refer to De Grauwe and Ji (2020) and Hommes and Lustenhouwer (2019a).

standard deviations of $\sigma^x = 0.5$, $\sigma^\pi = 0.5$, and $\sigma^i = 0.5$. Results are averaged across multiple independent Monte Carlo iterations.

For the agent-based simulations, the default network structure is a scale-free Barabási–Albert network, which reflects empirical financial and social network properties with preferential attachment. This ensures that a small number of highly connected agents play a dominant role in expectation propagation. For sensitivity analysis, simulations are also conducted across four alternative network structures: (1) Scale-free (Barabási–Albert) network with 100 nodes and 1275 edges, (2) Small-world network with 1473 edges, (3) Random (Erdős-Rényi) network with 1200 edges, and (4) Regular lattice network with 3000 edges. These variations allow assessment of the robustness of results across different interaction topologies.

Table 2 outlines the parameters used, which are largely consistent with those in De Grauwe and Ji (2020, 2023).

Figure 2 presents the time series of the inflation rate, the corresponding market expectations, and the forecast errors from a representative simulation run with $\chi = 0.5$ over a simulation length of 200 periods.

4.2 Expectation dispersion across networks

To analyze agent susceptibility to network effects, computational experiments are conducted. Dispersion is defined as the cross-sectional standard deviation of inflation expectations and market sentiment. These experiments introduce distinct behavioral strategies: agents with degree centrality ranks (1st, 5th, 10th, and 25th) were seeded with either targeted or naive inflation expectations. The targeted strategy reflects a central bank's deliberate inflation narrative via highly central nodes, while the naive strategy illustrates the impact of distorting narratives. Agents update their expectations using a convex combination of heuristic-based forecasts and the weighted average of neighbors' expectations, modulated by the persuasion parameter χ. Following Eq. 20 in Sect. 3.5, agent i updates its forecast probability as:

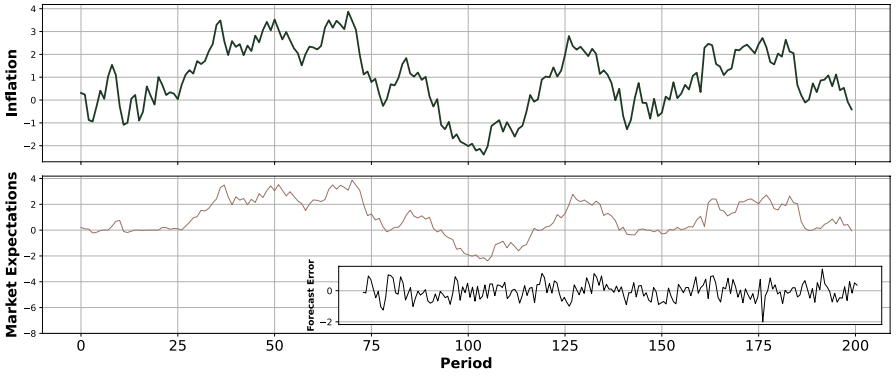

Fig. 2 *Inflation, Market Expectations, and Forecast Errors*. The top panel shows the evolution of inflation, the middle panel displays market expectations, and the inset highlights forecast errors

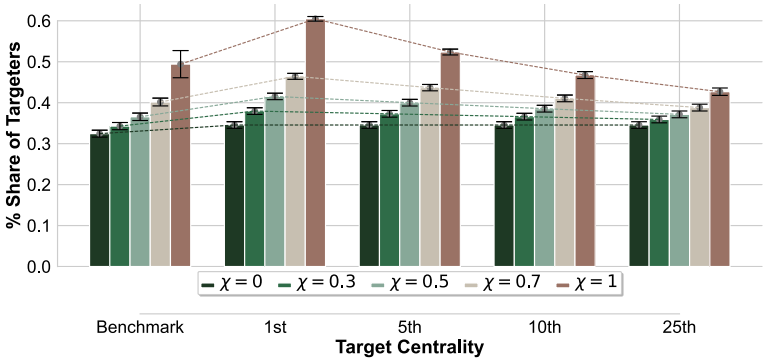

Fig. 3 *Average Share of Targeters in the Benchmark and under Targeted Intervention across Centrality Ranks (1st, 5th, 10th, 25th) for Persuasion Values (chi) varied in discrete steps (0, 0.3, 0.5, 0.7, 1).* Error bars indicate variability over 500 simulation iterations, each lasting 200 periods

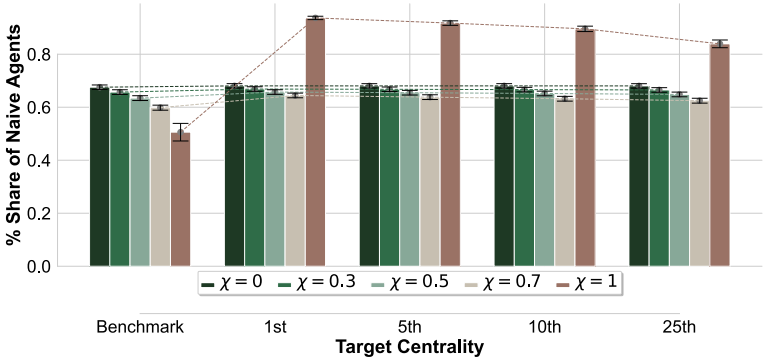

Fig. 4 *Average Share of Naive Agents in the Benchmark and under Naive Intervention across Centrality Ranks (1st, 5th, 10th, 25th) for Persuasion Values (chi) varied in discrete steps (0, 0.3, 0.5, 0.7, 1).* Error bars indicate variability over 500 simulation iterations, each lasting 200 periods

$$\omega_i^{k,j}(t) = \chi \cdot \left(\sum_{l=1}^{n} g_{il} \lambda_l^{k,j}(t-1) \right) + (1-\chi) \cdot \left(\frac{\exp\{\theta A_i^{k,j}(t)\}}{\sum_{j'} \exp\{\theta A_i^{k,j'}(t)\}} \right)$$

Here, χ determines the relative weight of the social conformity term (derived from the trust matrix interaction $\mathbb{T} \cdot \mathbb{I}_{t-1}^{k}$) versus the individual performance-based switching probability. For the main simulations, the Barabási–Albert scale-free network is employed. Results are read through the mechanism in §3.5: $\mathbb{T} \cdot \mathbb{I}_{t-1}^{k}$ concentrates mass on the heuristic adopted by hubs, and χ governs how strongly Ω_t^k maps this into aggregate beliefs. Highly connected agents thus significantly shape overall market expectations.

Figures 3 and 4 illustrate the impact of behavioral interventions on the mean share of inflation targeters and naive agents - grouped by degree centrality - as the persuasion parameter (χ) varies. When $\chi \neq 0$, significant differences emerge both within and across centrality groups. Under the targeted intervention, even agents

with lower centrality adopt target-based expectations more frequently as social influence strengthens (see Fig. 3). The nested heuristic switching model ($\chi = 0$) shows the lowest share of targeters, whereas the nested DeGroot model ($\chi = 1$) achieves the highest, which confirms that full network-based updating drives stronger convergence. For intermediate persuasion levels ($\chi = 0.3, 0.5, 0.7$), the mean share of targeters increases steadily with centrality—particularly between the 1st and 5th ranks—but this effect is less pronounced for agents ranked below 10th, indicating that highly central agents are more responsive to targeted narratives.

In contrast, in the naive intervention scenario (Fig. 4), the share of naive expectations increases significantly at $\chi = 1$ under the nested DeGroot model, exceeding even the effect observed under targeted interventions. For intermediate χ values (0.3, 0.5, 0.7), the increase in naive expectations is modest and shows little sensitivity to centrality, suggesting a uniformly destabilizing influence across the network.

Compared to targeted interventions, naive interventions exhibit smaller effect sizes and weaker differentiation across centrality ranks. While targeted interventions show pronounced increases in inflation targeters, particularly among highly central agents, naive interventions result in more evenly distributed effects. As χ rises, the share of naive expectations declines in the benchmark, whereas inflation targeters consistently increase.

Figures 5 and 6 illustrate the distribution and dispersion of market sentiment—calculated from the sentiment index (ranging from – 1 for purely deflationary to 1 for purely inflationary expectations) as defined in Eq. 14—across 500 Monte Carlo iterations. The sentiment index reflects the direction and degree of polarization or consensus in agents' inflation expectations during each simulation run. A lower mean dispersion indicates that most agents' inflation expectations are closely aligned, whether leaning toward inflation or deflation, resulting in a relatively narrow spread (high cohesion) of sentiment values over time. Conversely, a higher mean dispersion (e.g., 0.8) suggests that sentiment indices are more widely dispersed and volatile,

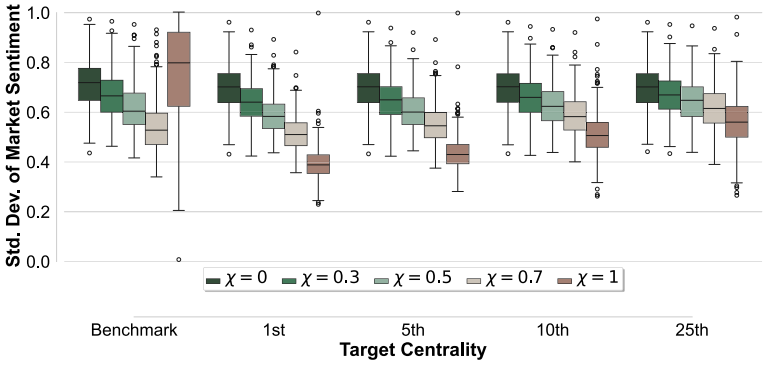

Fig. 5 *Dispersion of Inflation Market Sentiments in the Benchmark and under Targeted Intervention across Centrality Ranks (1st, 5th, 10th, 25th) for Persuasion Values (chi) varied in discrete steps (0, 0.3, 0.5, 0.7, 1).* Box plots show the average standard deviation of the sentiment index resulting from 500 Monte Carlo iterations each with 200 periods

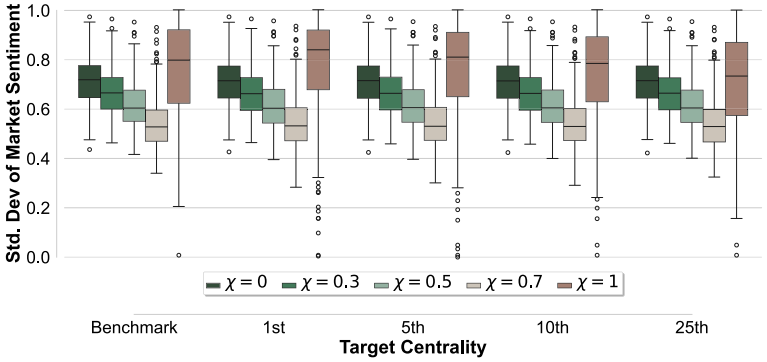

Fig. 6 *Dispersion of Inflation Market Sentiments in the Benchmark and under Naive Intervention across Centrality Ranks (1st, 5th, 10th, 25th) for Persuasion Values (chi) varied in discrete steps (0, 0.3, 0.5, 0.7, 1).* Box plots show the average standard deviation of the sentiment index resulting from 500 Monte Carlo iterations each with 200 periods

implying greater polarization and less anchored expectations. This increased divergence amplifies overall uncertainty in market expectations.

For targeted interventions (Fig. 5), the overall trend is an increase in the cohesion of market sentiment as persuasion levels rise, while the behavioral target intervention itself appears to have only a negligible effect (at least within the nested HSM and the integrated model) on market sentiments (see Fig. 5 for reference). However, in the absence of targeted anchoring, the nested DeGroot model exhibits a counterintuitive uptick in dispersion, with extreme persuasion ($\chi = 1$) seemingly increasing heterogeneity among agents. In contrast, the targeted intervention consistently maintains lower dispersion even at high persuasion levels, even for subordinate centrality ranks. This suggests that targeted messaging effectively narrows the range of sentiment, provided the agents' susceptibility to persuasion within the network is sufficiently high.

In contrast, the naive intervention (Fig. 6) exhibits a different pattern. Although sentiment dispersion declines as persuasion increases, mirroring the trend observed in the targeted case, the naive intervention appears to have minimal to no impact, particularly within the nested heuristic switching model and the integrated model. However, in the nested DeGroot model, the standard deviation rises at high persuasion levels and consistently remains elevated in the behavioral intervention scenarios, even for agents with lower centrality ranks.

4.3 Inflation dynamics and market stability

The analysis of behavioral interventions reveals a significant modulation of inflation dispersion, as quantified by the standard deviation of the inflation rate. Figures 7 and 8 present the variability of inflation under targeted and naive narrative interventions, with error bars capturing the distribution of standard deviations.

Figure 7 demonstrates that, under the target intervention scenario, the standard deviation of inflation consistently declines as the persuasion parameter (χ)

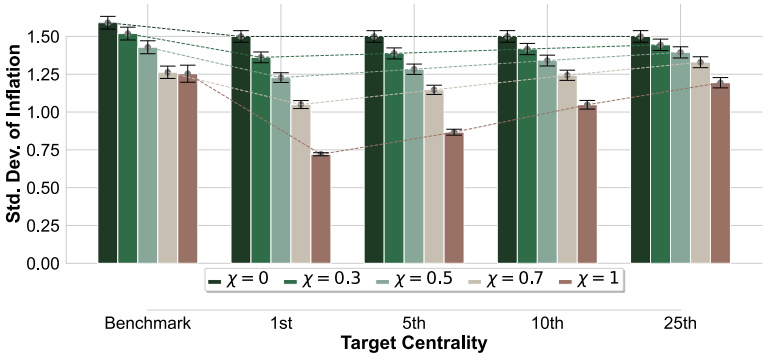

Fig. 7 *Average Inflation Dispersion in the Benchmark and under Target Intervention across Centrality Ranks (1st, 5th, 10th, 25th) for Persuasion Values (chi) varied in discrete steps (0, 0.3, 0.5, 0.7, 1).* Error bars indicate variability over 500 simulation iterations, each lasting 200 periods

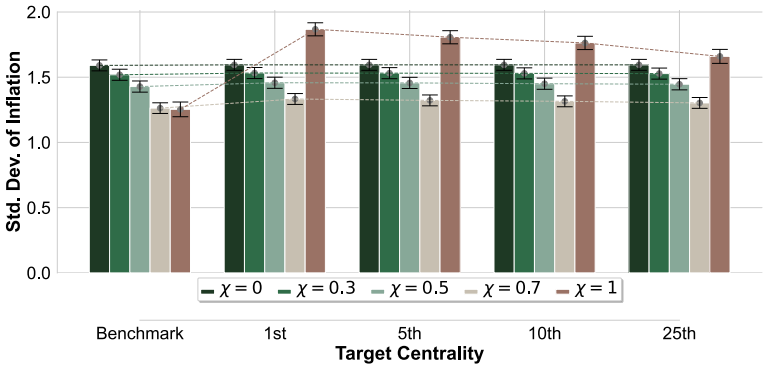

Fig. 8 Average Inflation Dispersion in the Benchmark and under Naive Intervention across Centrality Ranks (1st, 5th, 10th, 25th) for Persuasion Values (*chi*) varied in discrete steps (0, 0.3, 0.5, 0.7, 1). Error bars indicate variability over 500 simulation iterations, each lasting 200 periods

increases, with the most substantial reductions observed among agents with high degree centrality, particularly between the 1st and 5th ranks. This reduction indicates that when agents receive a targeted narrative aligned with the central bank's inflation target, their inflation expectations converge, leading to more stable inflation outcomes. In particular, under the nested DeGroot model ($\chi = 1$), where agents fully rely on network-based belief updating, the stabilization effect is most pronounced.

In contrast, the naive intervention (Fig. 8) demonstrates that only under the nested DeGroot model does a distorting narrative notably increase the standard deviation of the inflation rate, indicating that strong conformity pressures are necessary to significantly destabilize the market. In both the nested heuristic switching model (HSM) and the integrated model at intermediate persuasion levels ($\chi = 0.3$ and $\chi = 0.5$), the standard deviation remains relatively constant across different degree centrality ranks. This suggests that with moderate social influence, a naive narrative does not substantially affect inflation dispersion. However, when agents rely entirely on

network-based belief updating (i.e., $\chi = 1$ under the nested DeGroot model), an increase in dispersion is observed. Moreover, even among intermediate persuasion levels ($\chi = 0.3$, $\chi = 0.5$, and $\chi = 0.7$), subtle variations across centrality ranks appear, highlighting that the destabilizing impact of a naive narrative is sensitive to both the level of persuasion and agents' network positions.

Table 3 presents the estimated effects of behavioral interventions on the standard deviation of the inflation rate. The effect sizes are reported as Cohen's d (a standardized measure of the magnitude of the difference between the intervention and baseline scenarios) along with the corresponding t-statistics (with negative values indicating a reduction in the standard deviation relative to the benchmark) and the post hoc statistical power based on 500 simulation iterations.

For the targeted intervention, substantial reductions in the standard deviation of the inflation rate are observed at moderate to high levels of the persuasion parameter ($\chi = 0.3$, $\chi = 0.5$, and $\chi = 0.7$). Even agents with lower degree centrality (Rank 25) show statistically significant reductions, albeit with smaller effect sizes compared to more central agents. This finding implies that targeted dissemination of the central bank's inflation narrative can stabilize inflation outcomes across the network, benefiting even those agents who are less influential.

In contrast, the naive intervention displays a different pattern. At lower persuasion levels ($\chi \leq 0.7$), the effects on the standard deviation of inflation are minimal and statistically weak. However, when the persuasion parameter reaches its maximum value ($\chi = 1$), there is an increase in the standard deviation of the inflation rate. This increase is pronounced among agents with high degree centrality, but it also affects agents with lower centrality. This counterintuitive outcome—that a naive (or distorting) narrative can significantly destabilize inflation when social influence is very strong—underscores the potential risk such narratives pose to market stability when agents are highly susceptible to peer influence.

4.4 Dynamic responses (impulse analysis)

To compare the dynamic response of the model under rational expectations (RE) to its behavioral counterpart, I employ the method of undetermined coefficients. We assume linear solutions of the form

$$\pi_t = \psi_\pi^x \varepsilon_t^x + \psi_\pi^\pi \varepsilon_t^\pi + \psi_\pi^i \varepsilon_t^i, \qquad x_t = \psi_x^x \varepsilon_t^x + \psi_x^\pi \varepsilon_t^\pi + \psi_x^i \varepsilon_t^i,$$

substitute into the IS curve, NKPC, and Taylor rule, and solve for the coefficients by matching shock loadings in the IS curve, NKPC, and Taylor rule. Applying this method to the NK model defined in 3 yields, for a price shock at $t = 45$,

$$\psi_\pi^\pi = \frac{1}{1 + a_2 c_1 b_2}, \qquad \psi_x^\pi = \frac{-a_2 c_1}{1 + a_2 c_1 b_2}.$$

The detailed derivation is provided in in Appendix C.2. I use the RE solution strictly as a benchmark to interpret how χ alters convergence, not as a normative standard. Deviations from the RE path arise by construction from boundedly rational

Table 3 Estimated effect of varying persuasion parameter levels (χ) on the standard deviation of inflation, measured by T test differences relative to a baseline

		Target intervention		Naive intervention	
Persuasion	Centrality target	Est. effect	Post hoc power	Est. effect	Post hoc power
0	Rank 1	0.1833**	0.825	0.0094	0.053
		(−2.8977)		(0.148)	
	Rank 5	0.1837**	0.827	0.0092	0.052
		(−2.9047)		(0.146)	
	Rank 10	0.1827**	0.823	0.0094	0.053
		(−2.8893)		(0.149)	
	Rank 25	0.1829**	0.824	0.0093	0.052
		(−2.8920)		(0.147)	
0.3	Rank 1	0.3188***	0.999	0.0295	0.075
		(−5.0406)		(0.466)	
	Rank 5	**0.2607*** **	0.985	0.0273	0.072
		(−4.1217)		(0.432)	
	Rank 10	**0.1967****	0.874	0.0241	0.067
		(−3.1105)		(0.382)	
	Rank 25	**0.1356***	0.572	0.0198	0.061
		(−2.1443)		(0.313)	
0.5	Rank 1	0.4043***	1.000	0.0646	0.175
		(−6.3925)		(1.021)	
	Rank 5	**0.2776*** **	0.992	0.0609	0.161
		(−4.3898)		(0.963)	
	Rank 10	**0.1499***	0.658	0.0479	0.118
		(−2.3697)		(0.758)	
	Rank 25	0.0315	0.079	0.0381	0.092
		(−0.4975)		(0.602)	
0.7	Rank 1	0.4418***	1.000	0.1548*	0.686
		(−6.9853)		(2.447)	
	Rank 5	**0.2048****	0.899	**0.1296***	0.535
		(−3.2375)		(2.049)	
	Rank 10	0.0165	0.058	0.1135	0.434
		(0.261)		(1.795)	
	Rank 25	**0.2054****	0.901	0.0864	0.276
		(3.248)		(1.366)	
1.0	**Rank 1**	0.8460***	1.000	**1.0544*** **	**1.000**
		(−13.375)		(16.672)	
	Rank 5	0.5388***	1.000	**0.9696*** **	**1.000**
		(−8.5185)		(15.331)	
	Rank 10	0.1858**	0.835	**0.7502*** **	**1.000**
		(−2.9372)		(11.862)	
	Rank 25	0.0806	0.247	**0.7502*** **	**1.000**
		(−1.275)		(11.862)	

Table 3 (continued)

Persuasion	Centrality target	Target intervention		Naive intervention	
		Est. effect	Post hoc power	Est. effect	Post hoc power
Iterations		500		500	

The column *Est. Effect* reports Cohen's d, a standardized measure of the magnitude of the difference in inflation rate dispersion between intervention and benchmark scenarios. While Cohen's d is always positive, the direction of the effect is indicated by the sign of the t-statistic (reported in parentheses); negative t-statistics denote reduced inflation rate dispersion under intervention relative to the benchmark, and positive values denote increased dispersion. *Post hoc power* indicates the approximate probability of detecting an effect of this magnitude at the 5% significance level given 500 independent simulation runs (Monte Carlo iterations). Significance levels: $^{***}\ p < 0.01$, $^{**}\ p < 0.05$, $^{*}\ p < 0.10$

heuristic switching; the persuasion parameter χ then modulates these deviations by compressing or preserving dispersion through social interaction. Intuitively, higher χ puts more weight on the row-stochastic conformity operator, which contracts forecast dispersion before aggregation into $\widetilde{E}_t(\cdot)$. With smaller and shorter-lived expectation errors feeding the IS/NKPC block, transition dynamics move closer to the RE benchmark, yielding lower peaks and faster decay of IRFs. Thus, differences from RE reflect bounded rationality and interaction effects, not changes in deep parameters.

Using these coefficients, I visualize the effects of a one-period price shock (twice the s.d. of inflation) at $t = 45$. For the behavioral model, IRFs are computed as differences between shocked and baseline trajectories (Lengnick and Wohltmann 2016):

$$\mathrm{IRF}(z) = z_t^s - z_t^b \tag{21}$$

where z_t^s is the time series after the shock, and z_t^b is the baseline time series without the shock both based on 1000 Monte Carlo simulation iterations.

Figure 9a shows inflation's response: when χ is low (0, 0.3), the peak is higher and the decay slower. As χ rises (0.5, 0.7, 1), the peak is lower and the decay more rapid, consistent with stronger dispersion compression before aggregation. Figure 9b displays market expectations: lower χ yields greater and more persistent deviations from the RE path; higher χ reduces the peak deviation and shortens the half-life, indicating faster alignment of forecasts. Quantitatively, the half-life of the deviation falls monotonically in χ. Overall, stronger social influence speeds consensus and reduces deviations from RE; improvements are incremental between $\chi = 0.5, 0.7, 1$.

4.5 Sensitivity and robustness

The sensitivity analysis provides further evidence that increasing the persuasion parameter, χ, exerts a stabilizing influence on inflation dynamics. This analysis was conducted under the rationale of the behavioral intervention in which the central bank's inflation target is actively disseminated among agents. As illustrated in Figs. 10, 11, 12 and 13, the average dispersion of the inflation rate (measured as

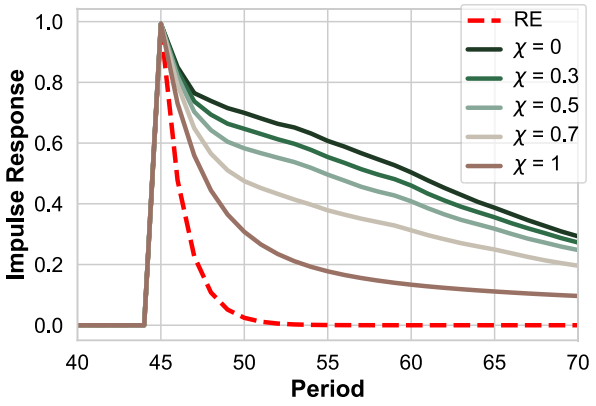

a Impulse Response of Inflation to a One-Period Price Shock at $t = 45$ (RE and Persuasion Values: 0, 0.3, 0.5, 0.7, 1)

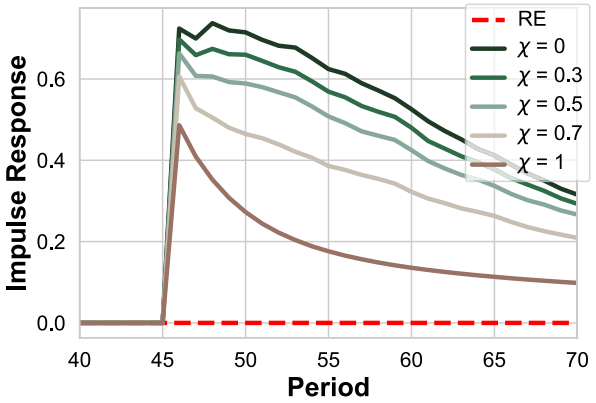

b Impulse Response of Market Expectations to a One-Period Price Shock at $t = 45$ (RE and Persuasion Values: 0, 0.3, 0.5, 0.7, 1)

Fig. 9 Overall impulse response analysis based on 1000 Monte Carlo simulation iterations. Panel **a** shows the response of inflation while panel **b** depicts the reaction of market expectations. Across panels, higher persuasion (χ) yields smaller IRF peaks and shorter half-lives, indicating faster convergence toward the RE benchmark

the standard deviation across simulation runs) declines consistently with higher χ values. This stabilizing effect is evident across multiple network structures. In both scale-free (Albert–Barabási; Fig. 10) and small-world (Watts–Strogatz; Fig. 11) networks, agent centrality significantly modulates the reduction in inflation dispersion, indicating that highly central agents contribute disproportionately to the stabilization effect. In contrast, random (Fig. 12) and regular networks (Fig. 13) exhibit negligible centrality effects, with the greatest reduction in standard deviation observed in regular networks. Overall, these results underscore that both the network structure and the degree of persuasion play crucial roles in shaping inflation dynamics. In particular, scale-free and small-world networks demonstrate

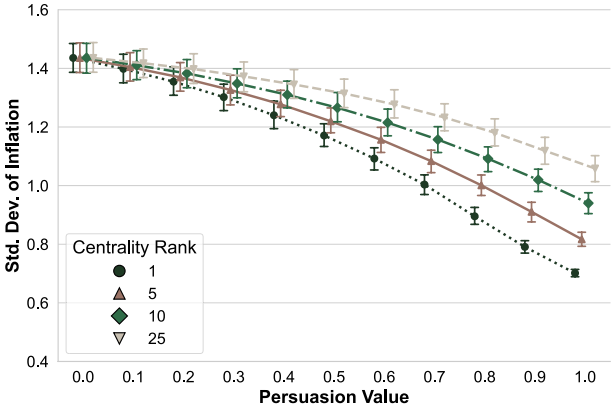

Fig. 10 *Sensitivity of Inflation Dispersion to Persuasion in a Scale-Free Network across Centrality Ranks (1st, 5th, 10th, 25th)* The x-axis shows χ, and the y-axis shows the average standard deviation of inflation. Results are averaged over 250 simulations

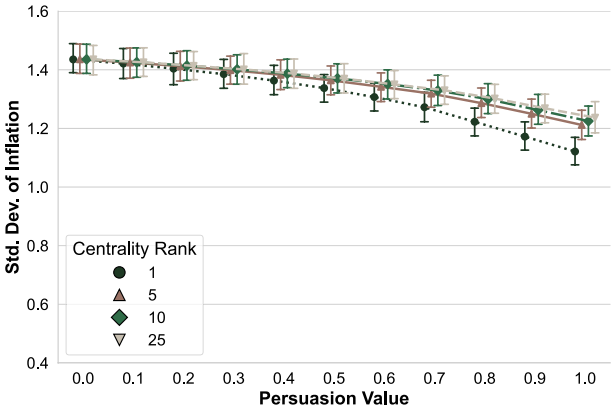

Fig. 11 *Sensitivity of Inflation Dispersion to Persuasion in a Small-World Network across Centrality Ranks (1st, 5th, 10th, 25th)* The x-axis shows χ, and the y-axis shows the average standard deviation of inflation. Results are averaged over 250 simulations

pronounced sensitivity to persuasion, with central agents acting as key conduits for information dissemination and belief updating, while random and regular networks display a more uniform behavior, suggesting a less pronounced influence of individual agents in these settings.

The sensitivity analysis is also conducted on the mean inflation rates, averaged over 250 Monte Carlo iterations. The findings indicate that as the persuasion parameter increases, the inflation rates converge to a steady-state value of zero, with progressively narrower confidence intervals. However, no significant differences are observed across targeted centrality ranks or between different network structures.

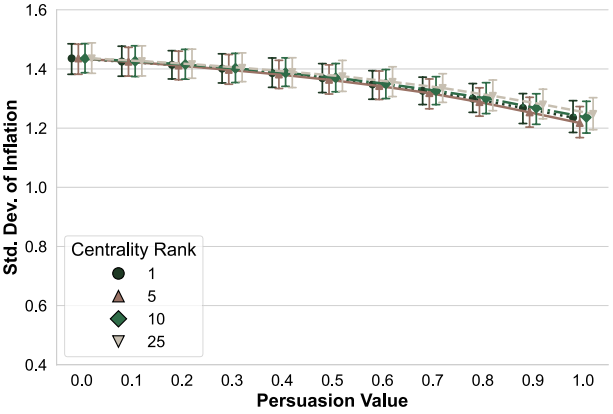

Fig. 12 *Sensitivity of Inflation Dispersion to Persuasion in a Random Network across Centrality Ranks (1st, 5th, 10th, 25th)* The x-axis shows χ, and the y-axis shows the average standard deviation of inflation. Results are averaged over 250 simulations

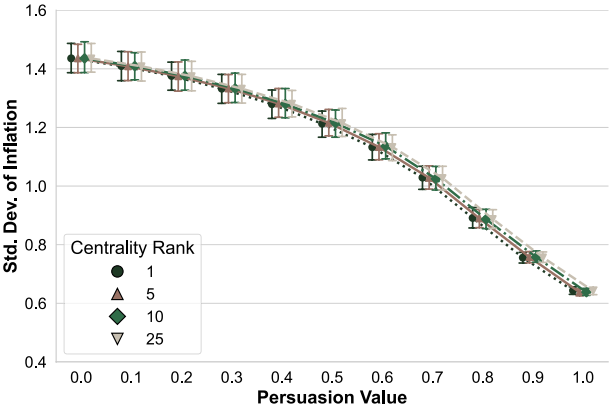

Fig. 13 *Sensitivity of Inflation Dispersion to Persuasion in a Regular Network across Centrality Ranks (1st, 5th, 10th, 25th)* The x-axis shows χ, and the y-axis shows the average standard deviation of inflation. Results are averaged over 250 simulations

Although these results are not included in the main text or abstract, they are available upon request.

Complementary to the analysis of inflation rate dispersion, I examine the sensitivity of the correlation between realized inflation and market sentiment to variations in χ. Recall that the sentiment index (ranging from -1 for purely deflationary to 1 for purely inflationary expectations) captures both the direction and degree of polarization or consensus among agents. A higher correlation between realized inflation and market sentiment indicates that agents' expectations are more closely anchored to the actual inflation outcomes.

Figure 14 presents the correlation coefficients between realized inflation and market sentiment across different values of χ, averaged over 500 Monte Carlo iterations (each spanning 200 simulation periods) for the Albert–Barabási network.

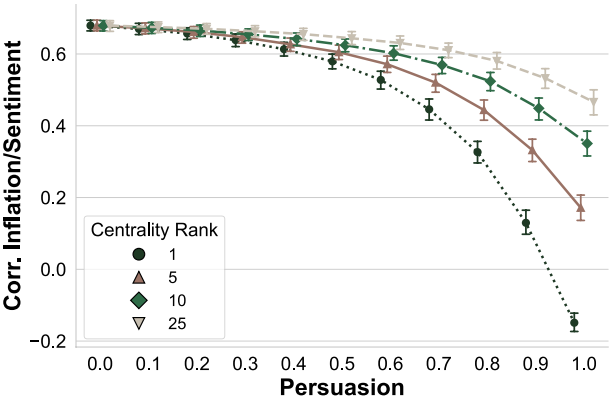

Fig. 14 Correlation between Realized Inflation and Sentiment Index in a Scale-Free Network across Persuasion Values for Centrality Ranks (1st, 5th, 10th, 25th). The x-axis shows χ, and the y-axis shows the average correlation coefficients. Results are averaged over 250 simulations

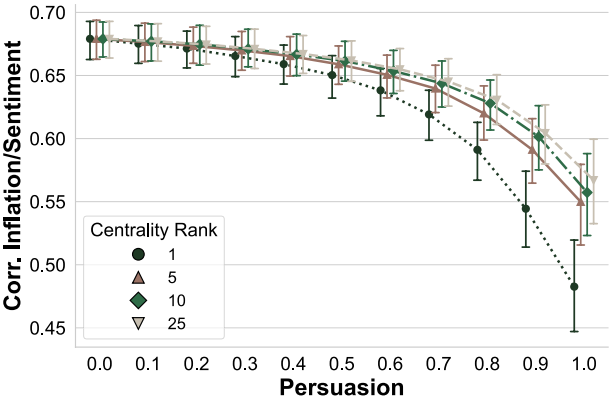

Fig. 15 Correlation between Realized Inflation and Sentiment Index in a Small-World Network across Persuasion Values for Centrality Ranks (1st, 5th, 10th, 25th). The x-axis shows χ, and the y-axis shows the average correlation coefficients. Results are averaged over 250 simulations

As χ increases, the correlation weakens, suggesting that higher persuasion levels diminish the alignment of agents' expectations with realized inflation. This trend is particularly pronounced in the Albert–Barabási network, where the correlation even turns negative when targeting the most central node with the behavioral target intervention.

A similar trend appears in the Watts–Strogatz small-world network, as shown in Fig. 15. Here, the correlation decreases with increasing χ, but the differences among agents at the 5th, 10th, and 25th centrality ranks remain negligible. However, a pronounced divergence emerges between the 1st and 5th ranks, indicating that the most central agents are more susceptible to persuasion, leading to a stronger divergence in their expectations relative to less central agents.

In contrast, the random network, depicted in Fig. 16, exhibits a muted response in the correlation between inflation and sentiment as χ increases. This uniformity in

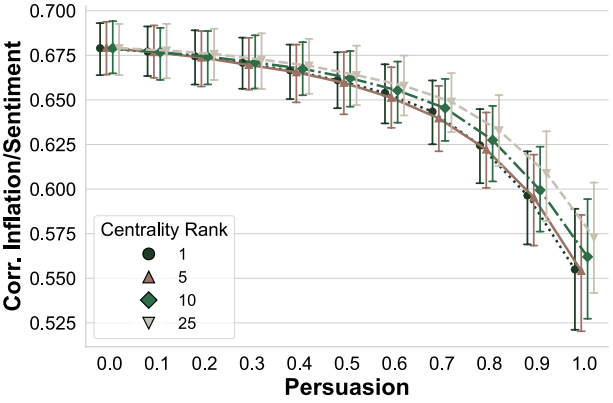

Fig. 16 Correlation between realized inflation and Sentiment Index in a Random Network across Persuasion Values for Centrality Ranks (1st, 5th, 10th, 25th). The x-axis shows χ, and the y-axis shows the average correlation coefficients. Results are averaged over 250 simulations

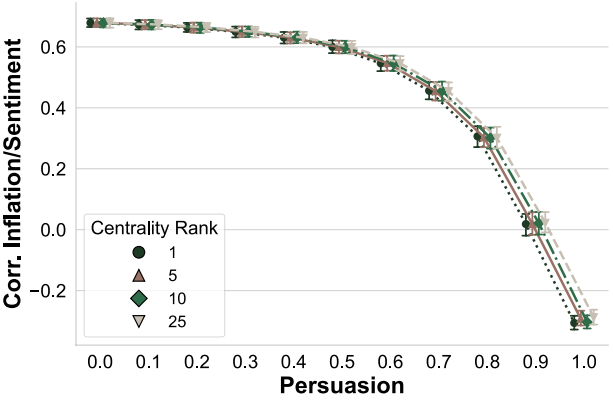

Fig. 17 Correlation between realized inflation and Sentiment Index in a Regular Network across Persuasion Values for Centrality Ranks (1st, 5th, 10th, 25th). The x-axis shows χ, and the y-axis shows the average correlation coefficients. Results are averaged over 250 simulations

influence ensures negligible differences across centrality ranks, aligning with theoretical expectations about the even distribution of influence in random networks. This homogeneity results in a more consistent response to changes in persuasion, reflecting the network's structural properties.

The regular network, as shown in Fig. 17, demonstrates a strong responsiveness of the inflation–sentiment correlation to increasing persuasion similarly. At higher χ levels, the correlation even turns negative, indicating a collective divergence between realized inflation and market sentiment. This behavior is reminiscent of the dynamics observed in the Albert–Barabási scale-free network (Fig. 14), where the correlation also becomes negative at high persuasion levels, particularly when targeting the most central node with the behavioral target intervention. Unlike the scale-free and small-world networks, however, no significant differences emerge

across centrality ranks in the regular graph. This uniformity underscores the homogeneous structure of regular networks, where all agents exert similar influence, leading to a network-wide shift in expectation formation as persuasion intensifies.

5 Discussion

A central contribution of this study is the integration of behavioral heuristics with network-mediated belief updating, organized around the persuasion parameter χ. This parameter bridges the heuristic switching model ($\chi = 0$) and the DeGroot network model ($\chi = 1$), allowing agents to be influenced by both forecasting performance and social conformity. The macrolevel consequences are conditional on the narrative environment: when the central bank's target heuristic diffuses through hubs, higher χ compresses dispersion, stabilizes inflation, and accelerates convergence; when naive heuristics spread, destabilization arises only at very high χ. The dispersion mechanism implies this conditional effect, while impulse response functions are consistent with the proposed mechanism, showing faster convergence and reduced forecast heterogeneity at higher χ.

The model's predictions resonate well with documented mechanisms. Forecasts are not formed in isolation but continuously adjusted to peers, producing herd behavior and shock amplification (Bargigli and Tedeschi 2014; Bailey et al. 2018). Reliance on social cues is pervasive in economic decision-making under uncertainty, where heuristic imitation and conformity biases shape expectations (Charness et al. 2013; Arrondel et al. 2022). Strong conformity can sustain beliefs even against fundamentals, as seen in filter bubbles or bot-driven amplification (Flynn and Sastry 2025). The decline in the inflation–sentiment correlation at higher χ mirrors this detachment, highlighting the double-edged role of central agents: persuasion narrows dispersion and stabilizes dynamics, yet simultaneously risks decoupling expectations from fundamentals (Corazzini et al. 2012). This detachment may weaken central bank credibility and trigger self-reinforcing expectation cycles, consistent with evidence that investors rely on socially transmitted information (Ivković and Weisbenner 2007; Oldham 2019).

The results also highlight dual channels of heterogeneity. First, agents differ by forecasting strategy (target-based vs. naive), which evolve with past performance. Second, agents differ structurally by network position (central vs. peripheral). This dual heterogeneity explains why convergence can coexist with persistent biases, depending on topology and narrative content. These findings align with opinion dynamics research showing that social learning can foster both consensus and fragmentation (Hong et al. 2004; Han and Yang 2013; DeGroot 1974). Recent work further shows that heterogeneous activity levels slow consensus (Li and Porter 2023). Consistent with these mechanisms, central nodes in the simulation amplify dominant heuristics, while variation in exposure conditions the persistence of biased beliefs.

Finally, the model relies on deliberate structural abstractions. First, it abstracts from narrative content to isolate diffusion strength: agents follow simplified belief rules rather than evolving stories. Second, the network layer uses canonical topologies (scale-free, small-world, random, regular) as isolation devices (Mäki

2009) to identify how hubness and clustering interact with persuasion. Third, a deliberate conceptual tension is maintained between the behavioral agents and the structural core. Embedding socially transmitted heuristics in a New Keynesian scaffold juxtaposes bounded rationality with equilibrium conditions derived from representative-agent optimization. As noted in Sect. 3, this is a methodological choice: by fixing the macroscaffold as a comparative benchmark, the analysis isolates the marginal effect of network dynamics without the confounding effects of wealth or fiscal dynamics inherent in fully microfounded aggregations.

Future work should relax these constraints. Cognitive and social heterogeneity, currently flattened by homogeneous parameters (χ, θ), could be expanded by introducing heterogeneous susceptibility $\{\chi_i, \theta_i\}$. Furthermore, adopting nonlinear influence mechanisms—such as bounded confidence, thresholds, or identity contagion—would allow the model to capture richer polarization dynamics. The network layer could also be extended beyond the canonical forms used here to include homophilic linkage based on agent characteristics (see, e.g., Schulz et al. 2022) or calibration using empirical networks, such as those derived from corporate board data (e.g., Vitali et al. 2011), to test the robustness of hub-driven stabilization. Finally, future research could endogenize macrorelations by embedding the framework in non-equilibrium structures (e.g., stock–flow consistent models) to allow endogenous macrostructures to emerge from microlevel social processes.

6 Concluding remarks

This paper examined how social interactions reshape the stability of macroeconomic expectations within a behavioral New Keynesian scaffold. By combining heuristic switching with network-mediated conformity, the framework isolates the role of persuasion and connectivity in amplifying or dampening belief dynamics.

Three broad insights emerge. First, anchoring effects are strongest when credible policy rules diffuse through central agents, compressing dispersion and lowering volatility. Second, destabilizing narratives matter only under very strong conformity, as performance-based learning tempers their impact at moderate persuasion. Third, social influence accelerates post-shock convergence but, when excessive, can weaken the link between expectations and fundamentals.

For policy, the message is double-edged. Network-aware communication that engages influential agents and sustains clear and consistent targets can anchor expectations and stabilize outcomes. However, these same structures may also amplify competing narratives, which can lead to misalignment and credibility loss.

The analysis is intentionally stylized: narratives are modeled as compact heuristics, persuasion is homogeneous, and networks are canonical rather than empirically calibrated. These simplifications sharpen the mechanism but narrow external validity. Future work should extend the framework with richer heterogeneity, nonlinear diffusion, and empirically grounded networks. In this sense, the model is best seen as a first step in identifying the incremental role of network structure in expectation formation and showing how persuasion and network topology interact with bounded rationality to shape macroeconomic stability.

Appendix A: Matrices

A.1: Indicator matrix

The indicator matrix, $\mathbb{I}_t^k \in \{0,1\}^{n\times 2}$, represents the forecasting decisions of all agents at time t for variable $k \in \{\pi, x\}$. Each row corresponds to an individual agent, while the two columns represent the two forecasting heuristics: target-based and static (naive). Specifically, it is defined as:

$$\mathbb{I}_t^k = \begin{bmatrix} \lambda_1^{k,\text{tar}}(t) & \left|\lambda_1^{k,\text{tar}}(t) - 1\right| \\ \lambda_2^{k,\text{tar}}(t) & \left|\lambda_2^{k,\text{tar}}(t) - 1\right| \\ \vdots & \vdots \\ \lambda_n^{k,\text{tar}}(t) & \left|\lambda_n^{k,\text{tar}}(t) - 1\right| \end{bmatrix} = (\lambda_i^k(t))_{i=1,..,n;k\in\{\pi,x\}} \; : \tag{A1}$$

Here, $\lambda_i^{k,\text{tar}}(t)$ denotes the forecasting decision of agent i for variable k: it equals 1 if the agent selects the target-based heuristic, and 0 otherwise. Consequently, $\left|\lambda_i^{k,\text{tar}}(t) - 1\right|$ equals 1 when the agent does not choose the target-based heuristic (i.e., when the static, or naive, heuristic is adopted). This formulation ensures that each agent's decision is fully captured by the two columns of $\mathbb{I}_t^k$.

A.2: Switching probabilities matrix (SPM)

The switching probabilities matrix, denoted as $\mathbb{B}_t^k$, captures the probabilities that agents switch between forecasting heuristics at time t for variable k. Each row corresponds to an agent, and the two columns correspond to the two heuristics: target-based (*tar*) and static (*stat*). We assume that all agents share the same switching probability distribution:

$$\beta_i^{k,j}(t) = \beta^{k,j}(t) \quad \forall\, i,$$

and define:

$$\mathbb{B}_t^k = \begin{bmatrix} \beta_1^{k,tar}(t) & \beta_1^{k,stat}(t) \\ \beta_2^{k,tar}(t) & \beta_2^{k,stat}(t) \\ \vdots & \vdots \\ \beta_n^{k,tar}(t) & \beta_n^{k,stat}(t) \end{bmatrix} = (\beta_i^{k,j}(t))_{i=1,..,n;k\in\{\pi,x\};j\in\{tar,stat\}} \tag{A2}$$

A.3: Conformity probability matrix

The conformity probability matrix, denoted as $\mathbb{C}_t^k$, reflects the influence of social interactions on agents' forecasting decisions. It is computed as the product of the trust matrix and the indicator matrix from the previous period:

$$CPM_t^k = \mathbb{C}_t^k = \mathbb{T} \cdot \mathbb{I}_{t-1}^k \tag{A3}$$

$$= \begin{bmatrix} g_{11}\lambda_1^{k,tar}(t-1) + g_{12}\lambda_2^{k,tar}(t-1) + ... + g_{1n}\lambda_n^{k,tar}(t-1) & A_{11}\lambda_1^{k,stat}(t-1) + \dots \\ \vdots & \vdots \\ g_{n1}\lambda_1^{k,tar}(t-1) + g_{n2}\lambda_2^{k,tar}(t-1) + ... + g_{nn}\lambda_n^{k,tar}(t-1) & \vdots \end{bmatrix} \tag{A4}$$

$$CPM_t^k = \begin{bmatrix} \gamma_1^{k,tar}(t) & \gamma_1^{k,stat}(t) \\ \gamma_2^{k,tar}(t) & \gamma_2^{k,stat}(t) \\ \vdots & \vdots \\ \gamma_n^{k,tar}(t) & \gamma_n^{k,stat}(t) \end{bmatrix} = (\gamma_i^{k,j}(t))_{i=1,..,n;k\in\{\pi,x\};j\in\{tar,stat\}} \tag{A5}$$

$$\mathbb{C}_t^k = \mathbb{T} \cdot \mathbb{I}_{t-1}^k.$$

Each element $\gamma_i^{k,j}(t)$ in $\mathbb{C}_t^k$ represents the aggregate influence from all of agent i's neighbors on the likelihood of adopting heuristic j for variable k at time t.

A.4: Weighted probability matrix

The weighted probability matrix, denoted as Ω_t^k, integrates two distinct models: the individual-based switching probabilities from the SPM and the network-based conformity effects from the CPM. This integration is achieved via a convex combination, governed by the persuasion parameter χ, ranging between 0 and 1, which modulates the balance between an agent's personal forecasting performance and the influence of their social network:

$$\Omega_t^k = \chi\, \mathbb{C}_t^k + (1-\chi)\, \mathbb{B}_t^k. \tag{A6}$$

Element-wise, this is expressed as: with

$$\omega_i^{k,j}(t) = \chi \cdot \gamma_i^{k,j}(t) + (1-\chi) \cdot \beta_i^{k,j}(t), \tag{A7}$$

e.g.,

$$\begin{bmatrix} \chi * \gamma_1^{k,tar}(t) + (1-\chi) * \beta_1^{k,tar}(t) & \chi * \gamma_1^{k,stat}(t) + (1-\chi) * \beta_1^{k,stat}(t) \\ \chi * \gamma_2^{k,tar}(t) + (1-\chi) * \beta_2^{k,tar}(t) & \chi * \gamma_2^{k,stat}(t) + (1-\chi) * \beta_2^{k,stat}(t) \\ \vdots & \vdots \\ \chi * \gamma_n^{k,tar}(t) + (1-\chi) * \beta_n^{k,tar}(t) & \chi * \gamma_n^{k,stat}(t) + (1-\chi) * \beta_n^{k,stat}(t) \end{bmatrix} \tag{A8}$$

$$= \begin{bmatrix} \omega_1^{k,tar}(t) & \omega_1^{k,stat}(t) \\ \omega_2^{k,tar}(t) & \omega_2^{k,stat}(t) \\ \vdots & \vdots \\ \omega_n^{k,tar}(t) & \omega_n^{k,stat}(t) \end{bmatrix} = (\omega_i^{k,j}(t))_{i=1,..,n;k\in\{\pi,x\};j\in\{tar,stat\}} \tag{A9}$$

where $\omega_i^{k,j}(t)$ is the effective switching probability for agent i to select heuristic j for variable k at time t. A higher χ value indicates greater reliance on social influence, whereas a lower χ reflects a higher confidence in individual judgment.

Appendix B: Simulation algorithms

Algorithm 2 Overall Model Simulation Process (Part I: Expectation Formation and Social Influence)

Require: Model parameters and initial conditions

- Number of agents N and simulation horizon T.
- Model parameters: a_1, a_2, b_1, b_2, c_1, c_2, c_3, π^*, ζ, θ, χ, and noise standard deviations σ^x, σ^π, σ^i.
- Initial macro variables: x_0, π_0, i_0.
- Initial expectation forecasts $\tilde{E}^j_{-1}(k)$ for $k \in \{x, \pi\}$ and $j \in \{\text{tar}, \text{stat}\}$.
- Network structure to generate the Trust Matrix $\mathbb{T}$, with elements g_{ij}.
- Initial indicator matrices $\mathbb{I}^k_0 \in \{0,1\}^{N\times 2}$ for $k \in \{x, \pi\}$.

Initialize:
Generate network and compute Trust Matrix $\mathbb{T}$.
Set initial indicator matrices $\mathbb{I}^\pi_0$, $\mathbb{I}^x_0$ (e.g., random assignment between target and naive).
Set x_0, π_0, i_0.
for $t = 1$ to T **do**
  for all $k \in \{x, \pi\}$ **do**
    for all agents $i = 1, \ldots, N$ **do**
      for all $j \in \{\text{tar}, \text{stat}\}$ **do**
        Compute forecast error:

$$\text{error}^j_i \leftarrow k_{t-1} - \tilde{E}^j_{t-2}(k_{t-1})$$

        Update attractiveness:

$$A^{k,j}_i(t) \leftarrow -\left(\text{error}^j_i\right)^2 + \zeta\, A^{k,j}_i(t-1)$$

        Compute individual switching probability:

$$\beta^{k,j}_i(t) \leftarrow \frac{\exp\{\theta\, A^{k,j}_i(t)\}}{\exp\{\theta\, A^{k,\text{tar}}_i(t)\} + \exp\{\theta\, A^{k,\text{stat}}_i(t)\}}$$

      end for
    end for
    for all agents $i = 1, \ldots, N$ **do**
      for all $j \in \{\text{tar}, \text{stat}\}$ **do**
        Compute social influence component:

$$\gamma^{k,j}_i(t) \leftarrow \sum_{l=1}^{N} g_{il}\, \lambda^{k,j}_l(t-1)$$

        Combine individual and social components:

$$\omega^{k,j}_i(t) \leftarrow \chi\, \gamma^{k,j}_i(t) + (1-\chi)\, \beta^{k,j}_i(t)$$

      end for
    end for

Algorithm 2 Overall Model Simulation Process (Part II: Matrix Aggregation and Macro-Updates)

Form the matrices:
Construct the Switching Probabilities Matrix $\mathbb{B}_t^k$ from $\{\beta_i^{k,j}(t)\}$.
Compute the Conformity Probabilities Matrix:

$$\mathbb{C}_t^k \leftarrow \mathbb{T} \cdot \mathbb{I}_{t-1}^k$$

Compute the Weighted Probabilities Matrix:

$$\Omega_t^k \leftarrow \chi\, \mathbb{C}_t^k + (1-\chi)\, \mathbb{B}_t^k$$

for all agents $i = 1, \ldots, N$ **do**
Draw a random outcome from $\{\text{tar}, \text{stat}\}$ using probabilities from the ith row of Ω_t^k.
Set indicator:

$$\lambda_i^{k,\text{tar}}(t) = \begin{cases} 1, & \text{if target heuristic is chosen} \\ 0, & \text{otherwise} \end{cases} \quad \text{and } \lambda_i^{k,\text{stat}}(t) = 1 - \lambda_i^{k,\text{tar}}(t).$$

end for
Update indicator matrix $\mathbb{I}_t^k$ accordingly.
Compute aggregate weights:

$$w_t^{k,\text{tar}} \leftarrow \frac{1}{N} \sum_{i=1}^{N} \lambda_i^{k,\text{tar}}(t), \quad w_t^{k,\text{stat}} \leftarrow 1 - w_t^{k,\text{tar}}.$$

Form market expectations:

$$\tilde{E}_t(k_{t+1}) \leftarrow w_t^{k,\text{tar}}\, k^* + w_t^{k,\text{stat}}\, k_{t-1},$$

where k^* is π^* for inflation and 0 for output gap.
end for
Update Macro Variables:
Update output gap using the New Keynesian IS curve:

$$x_t \leftarrow a_1\, \tilde{E}_t(x_{t+1}) + (1-a_1)x_{t-1} - a_2\Big(i_t - \tilde{E}_t(\pi_{t+1})\Big) + \epsilon_t^x.$$

Update inflation using the New Keynesian Phillips curve:

$$\pi_t \leftarrow b_1\, \tilde{E}_t(\pi_{t+1}) + (1-b_1)\pi_{t-1} + b_2 x_t + \epsilon_t^\pi.$$

Update nominal interest rate via the Taylor rule:

$$i_t \leftarrow (1-c_3)[c_1(\pi_t - \pi^*) + c_2 x_t] + c_3 i_{t-1} + \epsilon_t^i.$$

Generate noise terms ϵ_t^x, ϵ_t^π, ϵ_t^i as independent draws from $N(0, \sigma^x)$, $N(0, \sigma^\pi)$, $N(0, \sigma^i)$, respectively.
end for
return Time series of x_t, π_t, i_t and the evolution of indicator matrices $\mathbb{I}_t^k$, for $k \in \{x, \pi\}$.

Appendix C: Analytical solutions

C.1: Behavioral model solution

The solution of the behavioral model is found by substituting (3) into (1) as well as the forecasts specified in (21) and (22) into (1) and (2) and rewriting in matrix notation. This yields:

$$\underbrace{\begin{bmatrix} 1 + a_2c_2(1-c_3) & a_2c_1(1-c_3) \\ -b_2 & 1 \end{bmatrix}}_{\mathbb{A}} \underbrace{\begin{bmatrix} x_t \\ \pi_t \end{bmatrix}}_{\mathbb{Z}_t} =$$

$$\underbrace{\begin{bmatrix} 1 + a_1 w^{stat}_{x,t} - a_1 & w^{stat}_{\pi,t} \\ 0 & 1 + b_1 w^{stat}_{\pi,t} - b_1 \end{bmatrix}}_{\mathbb{B}_t} \underbrace{\begin{bmatrix} x_{t-1} \\ \pi_{t-1} \end{bmatrix}}_{\mathbb{Z}_{t-1}} +$$

$$+ \underbrace{\begin{bmatrix} a_2 w^{stat}_{\pi,t} - a_2c_1(c_3-1) \\ b_1 w^{tar}_{\pi,t} \end{bmatrix}}_{\mathbb{a}} \pi^* + \underbrace{\begin{bmatrix} -a_2c_3 \\ 0 \end{bmatrix}}_{\mathbb{b}} i_{t-1} + \underbrace{\begin{bmatrix} -a_2\epsilon^i_t + \epsilon^x_t \\ \epsilon^\pi_t \end{bmatrix}}_{\boldsymbol{\varepsilon}_t},$$

i.e.,

$$\mathbb{A}\mathbb{Z}_t = \mathbb{B}_t\mathbb{Z}_{t-1} + \mathbb{a}\boldsymbol{\pi}^* + \mathbb{b}\boldsymbol{i_{t-1}} + \boldsymbol{\varepsilon_t}$$

where bold characters refer to matrices and vectors. The solution for Z_t is given by

$$\mathbb{Z} \quad = \mathbb{A}^{-1}[\mathbb{B}\ \mathbb{Z}\ \_ \quad + \mathbb{a}\boldsymbol{\pi}^* + \mathbb{b}\boldsymbol{i_{t-1}} + \boldsymbol{\varepsilon_t}] \tag{C10}$$

The solution exists if the matrix $\mathbb{A}$ is non-singular; that is, if $(1 + a_2c_2(1-c_3)) + b_2a_2c_1(1-c_3) \neq 0$. The system describes the solutions for π_t and y_t. Finally, the solution for i_t is found by substituting x_t and π_t obtained from C10 into 3.

C.2: Impulse responses via method of undetermined coefficients

The demand side of the economy is represented by the New Keynesian IS curve:

$$x_t = a_1\tilde{E}_t(x_{t+1}) + (1-a_1)x_{t-1} - a_2(i_t - \tilde{E}_t(\pi_{t+1})) + \epsilon^x_t \tag{C11}$$

The supply side of the economy is described by the New Keynesian Phillips curve (NKPC):

$$\pi_t = b_1\tilde{E}_t(\pi_{t+1}) + (1-b_1)\pi_{t-1} + b_2x_t + \epsilon^\pi_t \tag{C12}$$

The central bank's response is modeled by the Taylor rule:

$$i_t = (1 - c_3)[c_1(\pi_t - \pi^*) + c_2 x_t] + c_3 i_{t-1} + \epsilon_t^i \tag{C13}$$

We assume that ϵ_t^x, ϵ_t^π, and ϵ_t^i follow a white-noise process, i.e.,

$$\begin{aligned} \epsilon_t^x &= \zeta_t \\ \epsilon_t^\pi &= \eta_t \\ \epsilon_t^i &= \xi_t \end{aligned} \tag{C14}$$

We make the following guesses for the solutions of π_t and x_t:

$$\begin{aligned} \pi_t &= \psi_\pi^x \epsilon_t^x + \psi_\pi^\pi \epsilon_t^\pi + \psi_\pi^i \epsilon_t^i \\ x_t &= \psi_x^x \epsilon_t^x + \psi_x^\pi \epsilon_t^\pi + \psi_x^i \epsilon_t^i \end{aligned} \tag{C15}$$

To determine the values of ψ_π^x, ψ_π^π, ψ_π^i, ψ_x^x, ψ_x^π, and ψ_x^i, we substitute the guesses and the random walk processes back into the IS equation:

$$\begin{aligned} \psi_x^x \epsilon_t^x + \psi_x^\pi \epsilon_t^\pi + \psi_x^i \epsilon_t^i = a_1 E_t(\psi_x^x \zeta_{t+1} + \psi_x^\pi \eta_{t+1} + \psi_x^i \xi_{t+1}) \\ + (1 - a_1) x_{t-1} - a_2 \big(i_t - E_t(\psi_\pi^x \zeta_{t+1} + \psi_\pi^\pi \eta_{t+1} + \psi_\pi^i \xi_{t+1})\big) + \epsilon_t^x \end{aligned}$$

Given that $E_t \zeta_{t+1} = E_t \eta_{t+1} = E_t \xi_{t+1} = 0$, this simplifies to:

$$\psi_x^x \epsilon_t^x + \psi_x^\pi \epsilon_t^\pi + \psi_x^i \epsilon_t^i = -a_2(c_1 \pi_t + c_2 x_t + \epsilon_t^i) + \epsilon_t^x$$

Collecting terms involving ϵ_t^x, ϵ_t^π, and ϵ_t^i to solve for the coefficients yields:

- For ϵ_t^x:

$$\psi_x^x = -a_2 c_2 \psi_x^x + 1$$

- For ϵ_t^π:

$$\psi_x^\pi = -a_2 c_1 \psi_\pi^\pi$$

- For ϵ_t^i:

$$\psi_x^i = -a_2 c_2 \psi_x^i + 1$$

Substituting the guesses and the random walk processes back into the NK Phillips curve yields:

$$\psi_\pi^x \epsilon_t^x + \psi_\pi^\pi \epsilon_t^\pi + \psi_\pi^i \epsilon_t^i = b_1 E_t(\psi_\pi^x \zeta_{t+1} + \psi_\pi^\pi \eta_{t+1} + \psi_\pi^i \xi_{t+1}) + b_2(\psi_x^x \epsilon_t^x + \psi_x^\pi \epsilon_t^\pi + \psi_x^i \epsilon_t^i) + \epsilon_t^\pi$$

Given that $E_t \zeta_{t+1} = E_t \eta_{t+1} = E_t \xi_{t+1} = 0$, this simplifies to:

$$\psi_\pi^x \epsilon_t^x + \psi_\pi^\pi \epsilon_t^\pi + \psi_\pi^i \epsilon_t^i = b_2(\psi_x^x \epsilon_t^x + \psi_x^\pi \epsilon_t^\pi + \psi_x^i \epsilon_t^i) + \epsilon_t^\pi$$

Collecting terms involving ϵ_t^x, ϵ_t^π, and ϵ_t^i to solve for the coefficients yields:

- For ϵ_t^x:

$$\psi_\pi^x = b_2\psi_x^x$$

- For ϵ_t^π:

$$\psi_\pi^\pi = b_2\psi_x^\pi + 1$$

- For ϵ_t^i:

$$\psi_\pi^i = b_2\psi_x^i$$

To solve for the coefficients ψ_x^x, ψ_x^π, ψ_x^i, ψ_π^x, ψ_π^π, and ψ_π^i, we equate the corresponding coefficients from the IS equation and the NK Phillips curve.

For ϵ_t^x:

From the IS equation:

$$\psi_x^x = -a_2c_2\psi_x^x + 1$$

From the NK Phillips curve:

$$\psi_\pi^x = b_2\psi_x^x$$

Substitute $\psi_\pi^x = b_2\psi_x^x$ into the IS equation:

$$\psi_x^x = -a_2c_2\psi_x^x + 1$$

$$\psi_x^x(1 + a_2c_2) = 1$$

$$\psi_x^x = \frac{1}{1 + a_2c_2} \tag{C16}$$

$$\psi_\pi^x = b_2\psi_x^x = \frac{b_2}{1 + a_2c_2} \tag{C17}$$

For ϵ_t^π:

From the IS equation:

$$\psi_x^\pi = -a_2c_1\psi_\pi^\pi$$

From the NK Phillips curve:

$$\psi_\pi^\pi = b_2\psi_x^\pi + 1$$

Substitute $\psi_\pi^\pi = b_2\psi_x^\pi + 1$ into the IS equation:

$$\psi_x^\pi = -a_2c_1(b_2\psi_x^\pi + 1)$$

$$\psi_x^{\pi}(1 + a_2c_1b_2) = -a_2c_1$$

$$\psi_x^{\pi} = \frac{-a_2c_1}{1 + a_2c_1b_2} \tag{C18}$$

$$\psi_{\pi}^{\pi} = b_2\psi_x^{\pi} + 1 = \frac{1}{1 + a_2c_1b_2} \tag{C19}$$

For ϵ_t^i

From the IS equation:

$$\psi_x^i = -a_2c_2\psi_x^i + 1$$

From the NK Phillips curve:

$$\psi_{\pi}^i = b_2\psi_x^i$$

Substitute $\psi_{\pi}^i = b_2\psi_x^i$ into the IS equation:

$$\psi_x^i(1 + a_2c_2) = 1$$

$$\psi_x^i = \frac{1}{1 + a_2c_2} \tag{C20}$$

$$\psi_{\pi}^i = b_2\psi_x^i = \frac{b_2}{1 + a_2c_2} \tag{C21}$$

To summarize, the coefficients are:

$$\psi_{\pi}^x = \frac{b_2}{1 + a_2c_2}$$
$$\psi_x^x = \frac{1}{1 + a_2c_2}$$
$$\psi_{\pi}^{\pi} = \frac{1}{1 + a_2c_1b_2}$$
$$\psi_x^{\pi} = \frac{-a_2c_1}{1 + a_2c_1b_2}$$
$$\psi_{\pi}^i = \frac{b_2}{1 + a_2c_2}$$
$$\psi_x^i = \frac{1}{1 + a_2c_2}$$

To derive the impulse response functions for a one-period shock to inflation, we proceed as follows:

1. Consider a one-period shock to inflation ϵ_t^π, e.g., $\eta_t = 1$. This means $\epsilon_t^\pi = 1$ at $t = 0$ and $\epsilon_t^\pi = 0$ for $t > 0$.
2. At $t = 0$, the shock affects π_0 and x_0 directly. Using the coefficients ψ_π^π and ψ_x^π:

$$\pi_0 = \psi_\pi^\pi \epsilon_0^\pi = \frac{1}{1 + a_2 c_1 b_2} \cdot 1$$

$$x_0 = \psi_x^\pi \epsilon_0^\pi = \frac{-a_2 c_1}{1 + a_2 c_1 b_2} \cdot 1$$

3. For $t > 0$, the shock ϵ_t^π returns to 0, but the model's dynamics will cause π_t and x_t to adjust over time based on the previous periods' values and the model's parameters.
4. Use the model equations to find the values in subsequent periods. Recall the equations:

$$x_t = a_1 \tilde{E}_t(x_{t+1}) + (1 - a_1) x_{t-1} - a_2(i_t - \tilde{E}_t(\pi_{t+1})) + \epsilon_t^x$$

$$\pi_t = b_1 \tilde{E}_t(\pi_{t+1}) + (1 - b_1)\pi_{t-1} + b_2 x_t + \epsilon_t^\pi$$

$$i_t = (1 - c_3)[c_1(\pi_t - \pi^*) + c_2 x_t] + c_3 i_{t-1} + \epsilon_t^i$$

   Given that $\epsilon_t^\pi = 0$ for $t > 0$, the impulse response will depend on the dynamics set in motion by the initial shock at $t = 0$.
5. For $t = 1$:

$$\pi_1 = b_1 E_1(\pi_2) + b_2 x_1$$

$$x_1 = E_1(x_2) - a_2(i_1 - E_1(\pi_2))$$

$$i_1 = (1 - c_3)[c_1(\pi_1 - \pi^*) + c_2 x_1] + c_3 i_{t-1}$$

   Given that $E_1(\pi_2)$ and $E_1(x_2)$ are the expected values based on the initial shock, use the known values of π_0 and x_0 to solve recursively for π_1 and x_1.
6. Repeat this process for $t = 2, 3, \ldots$, using the coefficients and recursive relationships to trace out the path of π_t and x_t.

Acknowledgements An earlier version of this paper was presented at the 29th International Conference Computing in Economics and Finance, Nice, France, July 3 to 6, 2023; the 26th and 27th Forum For Macroeconomics and Macroeconomic Policy, Berlin, Germany, October 20 to 22, 2022 and October 19 to 21, 2023; the BSE Summer Forum at the Workshop on Theoretical and Experimental Macroeconomics, Barcelona, Spain, June 12 to 13, 2023; the 26th Annual Workshop on Economic Science with Heterogeneous Interacting Agents, Koper, Slovenia, June 22 to 24, 2023; the 8th Meeting of the German Network for New Economic Dynamics, Gießen, Germany, October 4 to 6, 2022. I thank the participants, with special mention of Cars Hommes, John Duffy, Herbert Dawid, Rosemarie Nagel, Mikhail Anufriev, Valentyn Pachenko, Mikhail Pakhnin, Giorgio Ricchiuti, Jiří Kukačka, Giorgos Galanis, Chris Georges, Viktor Marinkov, Sylvain Barde and Mishel Ghassibe for their valuable comments. Additionally, I express my

sincere appreciation to Paul de Grauwe and David Andolfatto for their initial feedback. A special word of appreciation goes to my academic supervisor Frank Westerhoff and my colleagues Joep Lustenhouwer and Armin Aminian, who accompanied the creative process with thorough advice.

Author Contributions I confirm that I made substantial contributions to the conception and design of the work, the acquisition, analysis, and interpretation of data, and the drafting and critical revision of the manuscript. I approve the final version of the manuscript for publication and agree to be accountable for all aspects of the work, ensuring that any questions related to its accuracy or integrity are appropriately investigated and resolved.

Funding Open Access funding enabled and organized by Projekt DEAL. The author of this work was supported by a doctoral scholarship from the Hans Böckler Foundation, and their financial support is gratefully acknowledged. The views expressed in this research are solely those of the author and do not necessarily reflect the opinions of the Hans Böckler Foundation.

Data Availability The datasets generated and analyzed during the current study are not publicly available due to their proprietary nature but are available from the corresponding author upon request. The materials used in this study, including any supplementary files or additional documentation, are not publicly available but can be provided by the corresponding author upon request. The code used to generate the results and perform the analyses in this study is not publicly available but is available from the corresponding author upon request.

Declarations

Conflict of interest The authors declare no conflict of interest.

References

Acemoglu D, Carvalho VM, Ozdaglar A et al (2012) The network origins of aggregate fluctuations. Econometrica 80(5):1977–2016

Akerlof GA, Snower DJ (2016) Bread and bullets. J Econ Behav Organiz 126:58–71

Amaral LAN, Scala A, Barthelemy M et al (2000) Classes of small-world networks. Proc Natl Acad Sci 97(21):11149–11152

Andre P, Haaland I, Roth C et al (2024) Narratives about the macroeconomy. SAFE working paper 426, Frankfurt a. M., https://doi.org/10.2139/ssrn.4947636, https://hdl.handle.net/10419/302567

Anufriev M, Hommes C (2012) Evolutionary selection of individual expectations and aggregate outcomes in asset pricing experiments. Am Econ J Microecon 4(4):35–64. https://doi.org/10.1257/mic.4.4.35

Aral S, Walker D (2012) Identifying influential and susceptible members of social networks. Science 337(6092):337–341

Arifovic J, Bullard J, Kostyshyna O (2013) Social learning and monetary policy rules. Econ J 123(567):38–76. https://doi.org/10.1111/j.1468-0297.2012.02525.x

Arrondel L, Calvo-Pardo H, Giannitsarou C et al (2022) Informative social interactions. J Econ Behav Organiz 203:246–263

Assenza T, Bao T, Hommes C et al (2014) Experiments on expectations in macroeconomics and finance. In: Duffy J (ed) Experiments in macroeconomics-research in experimental economics, vol 17. Emerald Group Publishing Limited, New York, pp 11–70. https://doi.org/10.1108/S0193-23062014000017002
Assenza T, Cardaci A, Gatti DD et al (2018) Policy experiments in an agent-based model with credit networks. Economics 12(1):20180047
Azzimonti M, Fernandes M (2023) Social media networks, fake news, and polarization. Eur J Polit Econ 76:102256
Bailey M, Cao R, Kuchler T et al (2018) The economic effects of social networks: evidence from the housing market. J Polit Econ 126(6):2224–2276. https://doi.org/10.1086/700073
Bao T, Hommes C, Pei J (2021) Expectation formation in finance and macroeconomics: a review of new experimental evidence. J Behav Exp Financ 32:100591
Baqaee DR, Farhi E (2019) The macroeconomic impact of microeconomic shocks: beyond Hulten's theorem. Econometrica 87(4):1155–1203
Barabási AL (2009) Scale-free networks: a decade and beyond. Science 325(5939):412–413
Bargigli L, Tedeschi G (2014) Interaction in agent-based economics: a survey on the network approach. Physica A 399:1–15. https://doi.org/10.1016/j.physa.2013.12.029
Baumann F, Lorenz-Spreen P, Sokolov IM et al (2021a) Emergence of polarized ideological opinions in multidimensional topic spaces. Phys Rev X 11(1):011012
Baumann U, Darracq Paries M, Westermann T et al (2021b) Inflation expectations and their role in eurosystem forecasting. Occasional paper series/European Central Bank 264
Beckert J (2016) Imagined futures: fictional expectations and capitalist dynamics. Harvard UP
Beckert J, Bronk R (2018) Uncertain futures: imaginaries, narratives, and calculation in the economy. Oxford University Press, Oxford
Beckers B, Kholodilin KA, Ulbricht D (2017) Reading between the lines: using media to improve german inflation forecasts. DIW Berlin Discussion Paper No 1665. https://doi.org/10.2139/ssrn.2970466
Benhammada S, Amblard F, Chikhi S (2021) An agent-based model to study informational cascades in financial markets. N Gener Comput 39(2):409–436. https://doi.org/10.1007/s00354-021-00133-3
Bertella MA, Silva JN, Correa AL et al (2021) The influence of confidence and social networks on an agent-based model of stock exchange. Complexity 2021:1–16
Blattner TS, Margaritov E (2010) Towards a Robust Monetary Policy Rule for the Euro Area. Working Paper Series No. 1210, European Central bank
Blinder AS, Ehrmann M, Fratzscher M et al (2008) Central bank communication and monetary policy: a survey of theory and evidence. J Econ Lit 46(4):910–945
Blinder AS, Ehrmann M, De Haan J et al (2024) Central bank communication with the general public: Promise or false hope? J Econ Lit 62(2):425–457
Born B, Ehrmann M, Fratzscher M (2014) Central bank communication on financial stability. Econ J 124(577):701–734
Boyd S, Diaconis P, Xiao L (2004) Fastest mixing Markov chain on a graph. SIAM Rev 46(4):667–689
Branch WA (2004) The theory of rationally heterogeneous expectations: evidence from survey data on inflation expectations. Econ J 114(497):592–621. https://doi.org/10.1111/j.1468-0297.2004.00233.x
Branch WA, McGough B (2010) Dynamic predictor selection in a new Keynesian model with heterogeneous expectations. J Econ Dyn Control 34(8):1492–1508. https://doi.org/10.1016/j.jedc.2010.03.012
Brazier A, Harrison R, King M et al (2008) The danger of inflating expectations of macroeconomic stability: heuristic switching in an overlapping-generations monetary model. Int J Central Bank 4(2):219–254
Brock WA, Hommes CH (1997) A rational route to randomness. Econometrica 65(5):1059–1095
Brock WA, Hommes CH (1998) Heterogeneous beliefs and routes to chaos in a simple asset pricing model. J Econ Dyn Control 22(8–9):1235–1274. https://doi.org/10.1016/S0165-1889(98)00011-6
Buechel B, Hellmann T, Klößner S (2015) Opinion dynamics and wisdom under conformity. J Econ Dyn Control 52:240–257. https://doi.org/10.1016/j.jedc.2014.12.006
Carroll CD (2003) Macroeconomic expectations of households and professional forecasters. Q J Econ 118(1):269–298. https://doi.org/10.1162/00335530360535207
Carvalho VM (2014) From micro to macro via production networks. J Econ Perspect 28(4):23–48
Casiraghi M, Perez LP (2022) Central bank communications. IMF Technical Assistance Handbook

Chandrasekhar AG, Larreguy H, Xandri JP (2020) Testing models of social learning on networks: evidence from two experiments. Econometrica 88(1):1–32. https://doi.org/10.3982/ECTA14407
Charness G, Karni E, Levin D (2013) Ambiguity attitudes and social interactions: an experimental investigation. J Risk Uncertain 46:1–25
Choi S, Gale D, Kariv S (2008) Sequential equilibrium in monotone games: a theory-based analysis of experimental data. J Econ Theory 143(1):302–330. https://doi.org/10.1016/j.jet.2008.03.001
Cieslak A, Schrimpf A (2019) Non-monetary news in central bank communication. J Int Econ 118:293–315
Clarida R, Gali J, Gertler M (2000) Monetary policy rules and macroeconomic stability: evidence and some theory*. Quart J Econ 115(1):147–180. https://doi.org/10.1162/003355300554692
Clemente GP, Grassi R, Pederzoli C (2020) Networks and market-based measures of systemic risk: the european banking system in the aftermath of the financial crisis. J Econ Interac Coord 15(1):159–181. https://doi.org/10.1007/s11403-019-00247-4
Coibion O, Gorodnichenko Y, Kumar S et al (2020) Inflation expectations as a policy tool? J Int Econ 124:103297
Coibion O, Gorodnichenko Y, Kumar S et al (2021) Do you know that i know that you know...? higher-order beliefs in survey data. Q J Econ 136(3):1387–1446
Coibion O, Gorodnichenko Y, Weber M (2022) Monetary policy communications and their effects on household inflation expectations. J Polit Econ 130(6):1537–1584
Corazzini L, Pavesi F, Petrovich B et al (2012) Influential listeners: an experiment on persuasion bias in social networks. Eur Econ Rev 56(6):1276–1288. https://doi.org/10.1016/j.euroecorev.2012.05.005
Currarini S, Matheson J, Vega-Redondo F (2016) A simple model of homophily in social networks. Eur Econ Rev 90:18–39
Dawid H, Delli Gatti D (2018) Agent-based macroeconomics. In: Handbook of computational economics, vol 4. Elsevier, pp 63–156. https://doi.org/10.1016/bs.hescom.2018.02.006
De Grauwe P (2011) Animal spirits and monetary policy. Econ Theor 47(2):423–457. https://doi.org/10.1007/s00199-010-0543-0
De Grauwe P, Foresti P (2020) Animal spirits and fiscal policy. J Econ Behav Organiz 171:247–263. https://doi.org/10.1016/j.jebo.2020.01.015
De Grauwe P, Foresti P (2023) Interactions of fiscal and monetary policies under waves of optimism and pessimism. J Econ Behav Organiz 212:466–481
De Grauwe P, Ji Y (2019) Inflation targets and the zero lower bound in a behavioural macroeconomic model. Economica 86(342):262–299. https://doi.org/10.1111/ecca.12261
De Grauwe P, Ji Y (2020) Structural reforms, animal spirits, and monetary policies. Eur Econ Rev 124:103395. https://doi.org/10.1016/j.euroecorev.2020.103395
De Grauwe P, Ji Y (2023) On the use of current and forward-looking data in monetary policy: a behavioural macroeconomic approach. Oxf Econ Pap 75(2):526–552
DeGroot MH (1974) Reaching a consensus. J Am Stat Assoc 69(345):118–121. https://doi.org/10.1080/01621459.1974.10480137
Dosi G, Fagiolo G, Roventini A (2009) The microfoundations of business cycles: an evolutionary, multi-agent model. In: Schumpeterian Perspectives on Innovation, Competition and Growth, pp 161–180
Dosi G, Fagiolo G, Roventini A (2010) Schumpeter meeting keynes: a policy-friendly model of endogenous growth and business cycles. J Econ Dyn Control 34(9):1748–1767
Dräger L (2023) Central bank communication with the general public. CESifo Working Paper Series (10713)
Dräger L, Gründler K, Potrafke N (2025) Peer effects in macroeconomic expectations. Technical report, CESifo working paper
Easaw J, Mossay P (2015) Households forming macroeconomic expectations: inattentive behavior with social learning. BE J Macroecon 15(1):339–363
Erdos P, Rényi A et al (1960) On the evolution of random graphs. Publ Math Inst Hung Acad Sci 5(1):17–60
Fagiolo G, Roventini A (2017) Macroeconomic policy in dsge and agent-based models redux: New developments and challenges ahead. J Artif Soc Soc Simul 20(1):1. https://doi.org/10.18564/jasss.3280
Farmer JD, Foley D (2009) The economy needs agent-based modelling. Nature 460(7256):685–686
Flynn JP, Sastry K (2024) The macroeconomics of narratives. NBER working paper 32602
Flynn J, Sastry K (2025) How animal spirits affect the economy. IMF F&D Magazine. https://www.imf.org/en/Publications/fandd/issues/2025/03/how-animal-spirits-affect-the-economy-karthik-sastry

Franke R, Westerhoff F (2018) Taking stock: a rigorous modelling of animal spirits in macroeconomics. In: Veneziani R, Zamparelli L (eds) Analytical political economy. Wiley, Oxford, pp 5–38. https://doi.org/10.1002/9781119483328.ch2
Gabaix X (2020) A behavioral new keynesian model. Am Econ Rev 110(8):2271–2327. https://doi.org/10.1257/aer.20162005
Galanis G, Kollias I, Leventidis I et al (2022) Generalizing heuristic switching models. AWI discussion paper series (No. 715)
Galí J (2008) Monetary policy, inflation, and the business cycle: an introduction to the new Keynesian framework. Princeton University Press, Princeton
Gigerenzer G, Selten R (2002) Bounded rationality: the adaptive toolbox. MIT Press, Cambridge
Golub B, Jackson MO (2010) Naive learning in social networks and the wisdom of crowds. Am Econ J Microecon 2(1):112–149
Golub B, Jackson MO (2012) How homophily affects the speed of learning and best-response dynamics. Q J Econ 127(3):1287–1338
Gorodnichenko Y, Pham T, Talavera O (2021) Social media, sentiment and public opinions: evidence from #Brexit and #USElection. Eur Econ Rev 136:103772. https://doi.org/10.1016/j.euroecorev.2021.103772
Granovetter M (1978) Threshold models of collective behavior. Am J Sociol 83(6):1420–1443
Hagenhoff T, Lustenhouwer J, Tsionas M (2025) The rationality bias. J Money Credit Bank 57(2–3):515–547
Han B, Yang L (2013) Social networks, information acquisition, and asset prices. Manag Sci 59(6):1444–1457. https://doi.org/10.1287/mnsc.1120.1678
Hatcher M, Hellmann T (2023) Communication, networks and asset price dynamics: a survey. J Econ Interact Coordin 1–58
Hegselmann R, Krause U (2002) Opinion dynamics and bounded confidence: models, analysis and simulation. J Artif Soc Soc Simul 5. https://api.semanticscholar.org/CorpusID:8130429
Hommes C (2011) The heterogeneous expectations hypothesis: some evidence from the lab. J Econ Dyn Control 35(1):1–24. https://doi.org/10.1016/j.jedc.2010.10.003
Hommes C (2013) Behavioral rationality and heterogeneous expectations in complex economic systems. Cambridge University Press, Cambridge. https://doi.org/10.1017/CBO9781139094276
Hommes C (2021) Behavioral and experimental macroeconomics and policy analysis: a complex systems approach. J Econ Lit 59(1):149–219
Hommes C, Lustenhouwer J (2019a) Inflation targeting and liquidity traps under endogenous credibility. J Monet Econ 107:48–62
Hommes C, Lustenhouwer J (2019b) Managing unanchored, heterogeneous expectations and liquidity traps. J Econ Dyn Control 101:1–16
Hommes C, Makarewicz T, Massaro D et al (2017) Genetic algorithm learning in a New Keynesian macroeconomic setup. J Evol Econ 27(5):1133–1155. https://doi.org/10.1007/s00191-017-0511-y
Hong H, Kubik JD, Stein JC (2004) Social interaction and stock-market participation. J Financ 59(1):137–163
Huang JP, Zhang Y, Wang J (2023) Dynamic effects of social influence on asset prices. J Econ Interac Coord 18(3):671–699
Iori G, Mantegna RN (2018) Empirical analyses of networks in finance. In: Handbook of computational economics, vol 4. Elsevier, pp 637–685. https://doi.org/10.1016/bs.hescom.2018.02.005
Ivković Z, Weisbenner S (2007) Information diffusion effects in individual investors' common stock purchases: covet thy neighbors' investment choices. Rev Financ Stud 20(4):1327–1357
Jackson MO et al (2008) Social and economic networks, vol 3. Princeton University Press, Princeton
Jadbabaie A, Molavi P, Sandroni A et al (2012) Non-Bayesian social learning. Games Econom Behav 76(1):210–225
Jang TS, Sacht S (2022) Macroeconomic dynamics under bounded rationality: on the impact of consumers' forecast heuristics. J Econ Interac Coord 17(3):849–873
Khashanah K, Alsulaiman T (2016) Network theory and behavioral finance in a heterogeneous market environment. Complexity 21(S2):530–554. https://doi.org/10.1002/cplx.21834
Lamla MJ, Vinogradov DV (2019) Central bank announcements: big news for little people? J Monet Econ 108:21–38
Lamla M, Vinogradov DV (2021) Is the word of a gentleman as good as his tweet? policy communications of the bank of england. Working paper series in economics 403, Lüneburg, https://hdl.handle.net/10419/234592

Larsen VH, Thorsrud LA, Zhulanova J (2021) News-driven inflation expectations and information rigidities. J Monet Econ 117:507–520
Lengnick M, Wohltmann HW (2016) Optimal monetary policy in a new Keynesian model with animal spirits and financial markets. J Econ Dyn Control 64:148–165. https://doi.org/10.1016/j.jedc.2016.01.003
Li GJ, Porter MA (2023) Bounded-confidence model of opinion dynamics with heterogeneous node-activity levels. Phys Rev Res 5(2):023179
Lorenz J (2007) Continuous opinion dynamics under bounded confidence: a survey. Int J Mod Phys C 18:1819–1838
Luan S, Reb J, Gigerenzer G (2019) Ecological rationality: fast-and-frugal heuristics for managerial decision making under uncertainty. Acad Manag J 62(6):1735–1759. https://doi.org/10.5465/amj.2018.0172
Luarn P, Yang JC, Chiu YP (2014) The network effect on information dissemination on social network sites. Comput Hum Behav 37:1–8. https://doi.org/10.1016/j.chb.2014.04.019
Lustenhouwer J (2021) Unanchored expectations: self-reinforcing liquidity traps and multiple steady states. Macroecon Dyn 25(4):845–873
Lux T, Westerhoff F (2009) Economics crisis. Nat Phys 5(1):2–3
Macaulay A, Song W (2023a) Narrative-driven fluctuations in sentiment: evidence linking traditional and social media. Technical report, Bank of Canada
Macaulay A, Song W (2023b) News media, inflation, and sentiment. AEA Pap Proc 113:172–176
MacKenzie D (2008) An engine, not a camera: How financial models shape markets. MIT Press, New York
Mäki U (2009) Missing the world. models as isolations and credible surrogate systems. Erkenntnis 70(1):29–43
Manski CF, McFadden D (eds) (1981) Structural analysis of discrete data with econometric applications. MIT Press, Cambridge
Martins AC (2008) Mobility and social network effects on extremist opinions. Phys Rev E Stat Nonlinear Soft Matter Phys 78(3):036104
Massaro D (2013) Heterogeneous expectations in monetary dsge models. J Econ Dyn Control 37(3):680–692
McFadden D (1974) Conditional logit analysis of qualitative choice behavior. Front Econom
Newman ME (2003) The structure and function of complex networks. SIAM Rev 45(2):167–256
Oldham M (2019) Understanding how short-termism and a dynamic investor network affects investor returns: an agent-based perspective. Complexity 2019:1–21. https://doi.org/10.1155/2019/1715624
Olfati-Saber R, Murray RM (2004) Consensus problems in networks of agents with switching topology and time-delays. IEEE Trans Autom Control 49(9):1520–1533
Onnela JP, Saramäki J, Hyvönen J et al (2007) Structure and tie strengths in mobile communication networks. Proc Natl Acad Sci 104(18):7332–7336
Panchenko V, Gerasymchuk S, Pavlov OV (2013) Asset price dynamics with heterogeneous beliefs and local network interactions. J Econ Dyn Control 37(12):2623–2642. https://doi.org/10.1016/j.jedc.2013.06.015
Pfajfar D, Žakelj B (2014) Experimental evidence on inflation expectation formation. J Econ Dyn Control 44:147–168. https://doi.org/10.1016/j.jedc.2014.04.012
Pfajfar D, Žakelj B (2018) Inflation expectations and monetary policy design: evidence from the laboratory. Macroecon Dyn 22(4):1035–1075
Proaño CR, Lojak B (2020) Animal spirits, risk premia and monetary policy at the zero lower bound. J Econ Behav Organiz 171:221–233
Rengs B, Scholz-Wäckerle M (2019) Consumption and class in evolutionary macroeconomics. J Evol Econ 29:229–263
Rengs B, Scholz-Wäckerle M, van den Bergh J (2020) Evolutionary macroeconomic assessment of employment and innovation impacts of climate policy packages. J Econ Behav Organiz 169:332–368
Roos M, Reccius M (2024) Narratives in economics. J Econ Surv 38(2):303–341
Schmitt N (2021) Heterogeneoues expectations and asset price dynamics. Macroecon Dyn 25(6):1538–1568. https://doi.org/10.1017/S1365100519000774
Schulz J, Mayerhoffer DM, Gebhard A (2022) A network-based explanation of inequality perceptions. Soc Netw 70:306–324

Selten R (1998) Features of experimentally observed bounded rationality. Eur Econ Rev 42(3–5):413–436. https://doi.org/10.1016/S0014-2921(97)00148-7
Sharpe SA, Sinha NR, Hollrah CA (2023) The power of narrative sentiment in economic forecasts. Int J Forecast 39(3):1097–1121
Shiller RJ (2017) Narrative economics. Am Econ Rev 107(4):967–1004. https://doi.org/10.1257/aer.107.4.967
Simon HA (1957) Models of man; social and rational. In: Models of man; social and rational. Wiley, Oxford, pp xiv, 287
Smets F, Wouters R (2003) An estimated dynamic stochastic general equilibrium model of the euro area. J Eur Econ Assoc 1(5):1123–1175. https://doi.org/10.1162/154247603770383415
Steinbacher M, Steinbacher M, Steinbacher M (2014) Interaction-based approach to economics and finance. In: Faggini M, Parziale A (eds) Complexity in economics: cutting edge research. Springer, Cham, pp 161–203. https://doi.org/10.1007/978-3-319-05185-7_10
Ter Ellen S, Larsen VH, Thorsrud LA (2022) Narrative monetary policy surprises and the media. J Money Credit Bank 54(5):1525–1549
Tuckett D, Nikolic M (2017) The role of conviction and narrative in decision-making under radical uncertainty. Theory Psychol 27(4):501–523
Tuckett D, Taffler R (2012) Fund management: an emotional finance perspective. CFA Institute Research Foundation, New York
Tuckett D, Tuckett D (2011) Minding the markets: an emotional finance view of financial instability. Springer, Berlin
Uzzi B, Spiro J (2005) Collaboration and creativity: the small world problem. Am J Sociol 111(2):447–504
Vitali S, Glattfelder JB, Battiston S (2011) The network of global corporate control. PLoS ONE 6(10):e25995
Watts DJ, Strogatz SH (1998) Collective dynamics of 'small-world'networks. Nature 393(6684):440–442
Will M, Groeneveld J, Frank K et al (2020) Combining social network analysis and agent-based modelling to explore dynamics of human interaction: a review. Socio-Environ Syst Model 2:16325–16325
Woodford M (2005) Central bank communication and policy effectiveness. Working Paper 11898, National Bureau of Economic Research. https://doi.org/10.3386/w11898